

The significance of nitrogen regeneration for new production within a filament of the Mauritanian upwelling system.

D. R. Clark¹, C. E. Widdicombe, A. P. Rees, E.M.S. Woodward.

Plymouth Marine Laboratory, Prospect Place, West Hoe, Plymouth, PL1 3DH. United Kingdom.

¹Author for correspondence drcl@pml.ac.uk Tel: (+44) 1752 633100

ABSTRACT

The Lagrangian progression of a biological community was followed in a filament of the Mauritanian upwelling system, North West Africa, during offshore advection. Inert dual tracers sulphur hexafluoride and helium-3 labelled a freshly upwelled patch of water that was mapped for 8 days. Changes in biological, physical and chemical characteristics were measured including phytoplankton productivity, nitrogen assimilation and regeneration. Freshly upwelled water contained high nutrient concentrations ($\text{NO}_3^- = 9.0 \pm 0.1 \mu\text{mol}\cdot\text{L}^{-1}$; $\text{PO}_4^{3-} = 0.7 \pm 0.1 \mu\text{mol}\cdot\text{L}^{-1}$; $\text{Si} = 2.7 \pm 0.1 \mu\text{mol}\cdot\text{L}^{-1}$) but was depleted in N compared to Redfield stoichiometry (N:P = 13.9:1). A maximum primary productivity rate of $0.7 \text{ molC}\cdot\text{m}^{-2}\cdot\text{d}^{-1}$ was measured on the continental shelf, associated with nitrogen assimilation rates of $43.8 \text{ nmol}\cdot\text{L}^{-1}\cdot\text{h}^{-1}$ for NO_3^- , $32.8 \text{ nmol}\cdot\text{L}^{-1}\cdot\text{h}^{-1}$ for NH_4^+ and a phytoplankton community dominated by diatoms and flagellates. Indicators of phytoplankton abundance and activity decreased as the labelled water mass transited the continental shelf slope into deeper water, possibly linked to the mixed layer depth exceeding the light penetration depth. By the end of the study, a primary productivity rate of $0.1 \text{ molC}\cdot\text{m}^{-2}\cdot\text{d}^{-1}$ was measured, associated with nitrogen assimilation rates of $3.9 \text{ nmol}\cdot\text{L}^{-1}\cdot\text{h}^{-1}$ for NO_3^- , $6.1 \text{ nmol}\cdot\text{L}^{-1}\cdot\text{h}^{-1}$ for NH_4^+ and lower nutrient concentrations ($\text{NO}_3^- = 4.6 \pm 0.3 \mu\text{mol}\cdot\text{L}^{-1}$; $\text{PO}_4^{3-} = 0.4 \pm 0.1 \mu\text{mol}\cdot\text{L}^{-1}$; $\text{Si} = 0.9 \pm 0.1 \mu\text{mol}\cdot\text{L}^{-1}$). Nitrogen regeneration and assimilation took place simultaneously; NH_4^+ was regenerated at $9.4\text{--}85.0 \text{ nmol}\cdot\text{L}^{-1}\cdot\text{h}^{-1}$; NH_4^+ was oxidised at $0.30\text{--}8.75 \text{ nmol}\cdot\text{L}^{-1}\cdot\text{h}^{-1}$; NO_2^- was oxidised at $25.55\text{--}81.11 \text{ nmol}\cdot\text{L}^{-1}\cdot\text{h}^{-1}$. Results highlight the importance of regenerated NH_4^+ in sustaining phytoplankton productivity and indicate that the upwelled NO_3^- pool contained an increasing fraction of regenerated NO_3^- as it advected offshore. By calculating this fraction and incorporating it into an f-ratio formulation we estimated that of the 12.38 TgC of annual regional production, 4.73 TgC was exportable.

1. Introduction

The combination of northeast trade winds and the Coriolis effect due to earth's rotation drives the upwelling of deep nutrient-rich waters into the photic zone of coastal regions in eastern ocean boundaries. Upwelling supports characteristically enhanced biological production and valuable ecosystem services typified by fisheries (Pauly and Christensen, 1995; Arístegui et al., 2009). The maturation and development of biological communities within upwelled water masses as they advect offshore reflects a characteristic feature of eastern boundary upwelling ecosystems (EBUE); the spatial separation of nutrient sources and sinks. Gauging the extent of biological production ultimately exported from upwelling regions is an area of continuing investigation and model development (Álvarez-Salgado et al., 2007; Arístegui et al., 2009).

1 The North West African upwelling system is possibly the least studied of the four global EBUE's
2 (California, Peru-Chile, Iberia/North West Africa, Benguela) and is potentially the most complex due to
3 its topography and circulation (Mittelstaedt, 1991; Tomczak and Godfrey, 2003; Arístegui et al., 2006,
4 Chavez and Messié, 2009; Meunier et al., 2012). The Mauritanian region within this system is
5 characterised by a relatively wide shelf area over which upwelled water influences biological
6 productivity (Mittelstaedt, 1991), while extended filaments and island induced eddies are additional
7 features (Arístegui et al., 2009). The system can be separated into two regimes; the region between
8 15°N and 20°N undergoes periodic upwelling which dominates during winter and spring, whereas the
9 region north of 20°N is characterised by year round coastal upwelling with maximum intensity during
10 summer and autumn (Mittelstaedt, 1991). The study region, located between 20-22°N, lies at the
11 confluence between the two source waters upwelled in this system (North Atlantic Central Water and
12 South Atlantic Central Water; Mittelstaedt, 1991), which differ in their salinity, temperature and
13 nutrient characteristics. Nutrient concentrations and potential rates of new production in this region are
14 towards the upper limits of the range reported for global EBUEs (Chavez and Messié, 2009).

15 The highly dynamic nature of upwelling systems challenges our ability to understand how biological
16 activity develops as water masses advect offshore, and what the implications of this activity are for C-
17 export. Both Eulerian (occupying a fixed location over time through which upwelled water passes) and
18 Lagrangian (occupying a water mass as it passes through space and time) strategies have been adopted.
19 The Eulerian approach was successfully applied in a study of the Northern Benguela by Postel et al.
20 (2014); a challenge facing this approach is the risk that stations do not sample successive changes in
21 upwelled water due to the dynamic meandering nature of advective transport. Drifting buoys have been
22 used in previous Lagrangian studies of upwelling regions (Joint et al., 2001b; Wilkerson and Dugdale,
23 1987) although buoy tracks diverge over time (D'Asaro, 2004) leading to uncertainty about the location
24 of upwelled water masses. To address some of these issues in the present study, the inert gases sulphur
25 hexafluoride (SF₆) and helium-3 (³He) were used to label a water body within a recently upwelled
26 filament (Nightingale et al., 2000). In combination with drifting buoys and mapping exercises, the
27 progression of this labelled water mass and its associated biological activity was followed in Lagrangian
28 mode during offshore advection. Our objective was to investigate phytoplankton productivity, microbial
29 nitrogen cycling and to estimate exportable new production.

30 The assimilation of nitrogen by phytoplankton was introduced as a means of estimating 'new',
31 'regenerated' and 'exportable' production (f-ratio; Dugdale and Goering, 1967; Eppley and Peterson,
32 1979), based on the assumption that NO₃⁻ regeneration and assimilation processes were spatially
33 distinct, being associated with the aphotic and photic zones respectively. Consequently, the physical
34 introduction of new nitrogen to the photic zone was deemed capable of supporting an increase in
35 phytoplankton productivity which was available for export. This was readily measured as NO₃⁻
36 assimilation, though included nitrogen derived from nitrogen fixation. All other forms of nitrogen were
37 deemed to be regenerated, having previously been subject to microbial activity and capable only of
38 sustaining rather than enhancing phytoplankton growth. This was readily measured as NH₄⁺ assimilation,
39 though included dissolved organic nitrogen (DON) forms. According to this concept, upwelling regions,
40 which characteristically introduced deep nutrient rich waters to the photic zone, were associated with
41 high f-ratios (i.e. >0.7) reflecting the high proportion of total nitrogen assimilation supported by NO₃⁻. By

1 contrast, strong stratification in oligotrophic gyres suppressed nutrient inputs to the photic zone and
2 biological competition for limited nutrient resources maintained very low NO_3^- concentrations and f-
3 ratios (i.e. <0.1).

4 Following the introduction of the new production paradigm it has been acknowledged that additional
5 sources and processes related to the biogeochemical cycling of nitrogen are important to new
6 production. Atmospheric inputs of nitrogen in oxidised, reduced and organic forms are significant for
7 oceanic productivity (Baker et al., 2003; Moore et al., 2013). The nitrogen inventory of regions such as
8 the North Atlantic is also influenced indirectly by atmospheric inputs, as iron associated with Saharan
9 dust enhances diazotrophic nitrogen fixation, a source of new nitrogen to the surface ocean (Moore et
10 al., 2009; Jickells and Moore, 2015). Although regenerated productivity has often been represented by,
11 and measured as, NH_4^+ assimilation, the significance of dissolved organic nitrogen (DON) as a substrate
12 for primary producers has become clearer, including the assimilation of urea and amino acids (Bronk
13 and Glibert, 1993; Bronk and Ward, 1999; Wafar et al., 2004; Moschonas et al., 2015). However, the
14 contribution to total production (i.e. the sum of 'new' and 'regenerated' production) provided by
15 organic forms of nitrogen are rarely considered in f-ratio calculations. A related issue is the active
16 release of DON following inorganic nitrogen assimilation; by being released from phytoplankton cells
17 rather than contributing to the formation of new cellular material (i.e. particulate organic nitrogen;
18 PON), this nitrogen is removed from the dissolved inorganic nitrogen pool but is not incorporated into
19 the measured rate of nitrogen assimilation using ^{15}N techniques (Bronk et al., 1994; Raimbault and
20 Garcia, 2008). Variability in the extent of DON release introduces error in the ^{15}N budgets of tracer
21 studies.

22 Error in measured rates of nitrogen assimilation is also introduced by concomitant processes which
23 regenerate nitrogen (Glibert et al., 1982; Kanda et al., 1987). $^{15}\text{NH}_4^+$ isotope dilution due to NH_4^+
24 regeneration was acknowledged in the new production paradigm while $^{15}\text{NO}_3^-$ isotope dilution due to
25 nitrification, the sequential oxidation of NH_4^+ to NO_2^- to NO_3^- by nitrifying microbes, was assumed to be
26 negligible within the photic zone (Dugdale and Goering, 1967). It has become clear that the process of
27 NH_4^+ regeneration in upwelling systems is highly significant (Raimbault and Garcia, 2008; Clark et al.,
28 2011; Fernández and Farías, 2012; Benevides et al., 2014); while zooplankton excretion and bacterial
29 remineralisation are important sources of NH_4^+ , mixotrophic nutrition may be a dominant strategy for
30 the plankton community in upwelling systems, which contribute to NH_4^+ regeneration (Benevides et al.,
31 2014; Mitra et al., 2014). A recently acknowledged role may also exist for the photochemical
32 degradation of DON which regenerates NH_4^+ within the sunlit ocean (Rain-Franco et al., 2014). The
33 combined influence of these processes provides a regenerative NH_4^+ flux which can equal or exceed sink
34 terms leading to sporadic NH_4^+ accumulation (Fernández and Farías, 2012). Consequently, the influence
35 of NH_4^+ regeneration upon isotope dilution needs to be accounted for in NH_4^+ assimilation rate
36 measurements and subsequent f-ratio calculations.

37 The inhibition of nitrification by light supported the assumption that nitrification was not an
38 important factor in f-ratio formulations for the photic zone (Olson, 1981). Although subsequent studies
39 have supported this distribution in nitrifying activity, measurements have demonstrated that NO_3^-
40 regeneration is significant when compared to concurrent NO_3^- assimilation in the photic zone
41 (Fernández et al., 2005, 2009; Fernández and Farías, 2012; Clark et al., 2011; 2014). Consequently,

1 although isotope dilution due to the regeneration of NO_3^- can be accounted for in NO_3^- assimilation rate
2 calculations, it is implicit that the surface ocean NO_3^- pool contains a fraction of regenerated NO_3^- which
3 cannot readily be measured directly (Martin and Pondaven, 2006).

4 Conceptually, improving the utility of f-ratio measurements would require a full consideration of all
5 new and regenerated forms of inorganic nitrogen to the photic zone which support primary
6 productivity. However, uncertainty about the fraction of photic zone NO_3^- that truly represents 'new'
7 NO_3^- is an important and conceptually fundamental limitation that has rarely been acknowledged.
8 Upwelling areas are an exceptional case; seawater upwelled in the Mauritanian system may be regarded
9 as genuinely 'new' to the photic zone, consistent with the original concept. Here we aimed to examine
10 the concept of a transition in NO_3^- pool provenance from 'new' towards 'regenerated' and to investigate
11 the implications for exportable production estimates in the Mauritanian Upwelling system.

12 13 **2. Materials and methods**

14 The study was undertaken on board the RRS Discovery (D338; 15th April to 27th May 2009) as a UK
15 contribution to the international Surface Ocean Lower Atmosphere Study (SOLAS) project. Remotely
16 sensed data was processed by NEODAAS at PML and used to identify a region of active upwelling.
17 Chlorophyll a data was received by NASA from MODIS and processed using the OC3 chlorophyll
18 algorithm in NASA's SeaWiFS software. Sea-surface temperature data was received by NOAA from
19 AVHRR and were processed using PML's in-house Panorama processing system (Miller et al., 1997).
20 Upwelling activity was confirmed by hydrographical surveys of water column physical structure involving
21 CTD rosette casts, Moving Vessel Profiler (MPV; incorporating CTD and fluorescence units) deployments
22 and the use of a shipboard Acoustic Doppler Current Profilers (ADCP; for full details of the mapping
23 exercise see Meunier et al. 2012). This data was used to select the position for drifter buoy deployment.
24 $\text{SF}_6/{}^3\text{He}$ was deployed in a patch (hereafter referred to as P_1) at a depth of 5m around the drifter; full
25 details of the dual tracer technique used during this research program are described in Nightingale et al.
26 (2000). The time interval between receiving satellite data and deploying $\text{SF}_6/{}^3\text{He}$ was < 2 days.

27 $\text{SF}_6/{}^3\text{He}$ was subsequently detected using two ship-based Gas Chromatography (GC) systems.
28 Seawater samples were collected in discrete mode from depth profiles using CTD rosette-mounted
29 Niskin bottles and continuous mode from the ships seawater supply collected at approximately 5m. This
30 analysis identified changes in the horizontal and vertical distribution of $\text{SF}_6/{}^3\text{He}$ marked seawater. It
31 ensured that seawater sampling for observational measurements was centred upon the labelled water
32 mass and that the same water mass was sampled until tracer concentrations could no longer be
33 detected reliably, due to the limits of detection associated with GC analysis. Using this approach,
34 chemical, physical and biological characteristics of the water mass were measured in Lagrangian mode.
35 The duration of the study was 8 days, with sequential sampling days identified by the notation T_0 - T_7 ;
36 pre-patch observations are referred to as T_{-1} . One day of sampling was lost due to challenging weather
37 conditions (T_5 , 28th April).

38 For nitrogen regeneration (NH_4^+ regeneration, NH_4^+ oxidation, NO_2^- oxidation) and nitrogen
39 assimilation (NH_4^+ , NO_2^- and NO_3^-) process measurements, seawater samples were collected from CTD
40 rosette-mounted Niskin bottles which sampled routinely at a depth equivalent to 55% of surface

1 photosynthetically active radiation (sPAR). Additional samples were taken from the 1% sPAR depth for
2 NO_2^- oxidation rate measurements only.

3 The assimilation and regeneration of DIN was investigated using ^{15}N amended seawater during deck
4 incubations (Clark et al., 2014). Simultaneously, size fractionated primary productivity was measured in
5 depth profiles using deck incubations with ^{14}C (Tilstone et al., 2009). For all deck incubations, neutral
6 density filters simulated sPAR according to Joint Global Ocean Flux Study protocols (Intergovernmental
7 Oceanographic Commission, 1994) and temperature control was achieved by flushing boxes with
8 seawater from the ships sea-surface supply collected at $\approx 5\text{m}$.

9 10 2.1 Nitrogen regeneration investigations.

11 A 24-position stainless steel rosette system was used to collect seawater from specific depths using
12 20 L Niskin bottles. Water columns were characterised during casts using additional instrumentation
13 attached to the rosette, which included Seabird 9 Plus conductivity, temperature, depth (CTD) units, a
14 Seabird SBE 43 dissolved oxygen sensor and a Chelsea MKIII Aquatracka fluorometer. Seawater was
15 collected during pre-dawn casts (approximately 04:00) at depths equivalent to specific sPAR values,
16 which were derived from the previous days light attenuation profiles. All glassware used for the
17 manipulation of seawater was cleaned with 10 % HCL (reagent grade, 37 %) between CTD sampling
18 iterations and rinsed thoroughly with Milli-Q high purity water within sampling iterations. Chemicals and
19 solvents were analytical and High Performance Liquid Chromatography (HPLC) grade respectively,
20 supplied by Sigma-Aldrich (UK) unless otherwise stated. Stable isotope salts ($^{15}\text{NH}_4\text{Cl}$, $\text{Na}^{15}\text{NO}_3$, $\text{Na}^{15}\text{NO}_2$)
21 were supplied by CK gas products Ltd (UK).

22 A 20 L volume of seawater from each sampling depth was collected in a blacked-out Nalgene
23 container. In the ships laboratory, the preparation of this seawater for incubation studies was also
24 undertaken using blacked-out containers to minimise sample exposure to artificial light sources and the
25 potential disruption of the biological community's natural light-dark cycle. Collected seawater was not
26 pre-filtered (i.e. to remove particles greater than a specific size). As an overview, 6 L of this seawater
27 was used for nitrogen assimilation studies while 12 L was used for nitrogen regeneration studies.
28 Generally, nitrogen regeneration studies were initiated prior to 09:00 GMT and terminated prior to
29 17:00 GMT providing an average incubation time of 8 hours. Within this incubation period, nitrogen
30 assimilation studies were generally initiated by 10:00 GMT and terminated by 16:00 GMT providing an
31 average incubation time of 6 hours. Incubations were therefore restricted to day-light hours.

32 NH_4^+ regeneration rate was determined by amending a 4 L volume of seawater in a blacked out
33 container with $^{15}\text{NH}_4^+$, achieving an average enrichment of $10.7 \pm 8.4\%$ $^{15}\text{NH}_4^+$. This volume was
34 thoroughly mixed and left to stand for 20 minutes in order to ensure homogeneity. Amended seawater
35 was used to fill a 2.2 L incubation bottle, which was placed in a deck incubator at simulated light and
36 temperature. The remaining amended seawater was filtered through GF/F glass fibre filters and
37 triplicate 100 mL volumes were set aside for the determination of pre-incubation NH_4^+ concentration
38 and isotopic enrichment by synthesising indophenol as described below. Following the deck incubation,
39 bottle contents were filtered through GF/F filters and the filtrate was distributed between 3 x 100 mL
40 volumes for the determination of post-incubation NH_4^+ concentration and isotopic enrichment by
41 synthesising indophenol.

1 A comparable procedure was used for NH_4^+ and NO_2^- oxidation incubations in which separate 4 L
2 volumes of seawater were amended with $^{15}\text{NO}_2^-$ and $^{15}\text{NO}_3^-$, achieving average ^{15}N enrichments of
3 $8.8\pm 0.9\%$ and $9.4\pm 0.9\%$ respectively. The concentration and isotopic enrichment of NO_2^- was
4 determined by synthesising sudan-1 in sample volumes of 100 mL, as described below. The
5 concentration and isotopic enrichment of NO_3^- was determined by first reducing NO_3^- to NO_2^- using a
6 high capacity cadmium column, and then synthesising sudan-1 in volumes of 25-50 mL varying with
7 ambient concentration.

8 Indophenol was synthesised in samples by adding the first reagent (4.7 g phenol and 0.32 g sodium
9 nitroprusside in 200 mL Milli Q water) in the proportion of 1 mL per 100 mL of sample volume, mixing
10 the sample and leaving for 5 minutes. The second reagent (1.2 g sodium dichloro-isocyanurate and 2.8 g
11 sodium hydroxide in 200 mL Milli Q) was then added in the proportion of 1 mL per 100 mL sample
12 volume, mixed and left for 8 hours at room temperature for indophenol development. Indophenol was
13 collected by solid-phase extraction (SPE). Sudan-1 was synthesised by adding the first reagent (0.8 g of
14 aniline sulphate in 200 mL 3M HCl) to samples in the proportion 0.5 mL per 100 mL sample volume.
15 Samples were mixed and left for 5 minutes to homogenise after which sample pH was verified to be \approx
16 2.0. Reagent 2 (24 g NaOH and 0.416 g 2-naphthol in 200 mL Milli Q) was added in the proportion 0.5 mL
17 per 100 mL sample volume. Samples were again mixed, left for 5 minutes before sample pH was verified
18 to be approximately 8.0. Sudan-1, the development of which was complete after 30 minutes of
19 incubation at room temperature, was collected by SPE.

20 Deuterated internal standards were added to samples immediately prior to SPE collection.
21 Deuterated indophenol and deuterated sudan-1 were synthesised according to methods described
22 previously (Clark et al., 2006; 2007) and purified by HPLC. Standard solutions in methanol were prepared
23 ($100 \text{ ng}\cdot\mu\text{L}^{-1}$) and the concentration verified against analytical standard solutions (Sigma-Aldrich).
24 Appropriate volumes of deuterated internal standards (i.e. comparable to sample size) were added to
25 samples following acidification by citric acid and prior to SPE collection.

26 Indophenol and sudan-1 were collected by SPE using 6 mL/500 mg C18 cartridges (Biotage, UK)
27 which were prepared for sample collection by first rinsing with 5 mL methanol, followed by 5 mL Milli Q
28 water and 5 mL 0.22 μm filtered seawater. Prior to sample collection seawater samples were acidified
29 with 1 M citric acid to a pH of 5.5, before collection by SPE under low vacuum (120 mmHg) at a flow rate
30 of approximately 1 mL per minute without drying. Samples were then rinsed with 5 mL 0.22 μm filtered
31 seawater and 5 mL Milli Q water before being air dried under high vacuum (360 mmHg). Samples were
32 stored frozen until further processing at the land based laboratory.

33 At the land based laboratory, samples were brought to room temperature and prepared for HPLC
34 purification and Gas Chromatography Mass Spectrometry (GCMS) analysis in the following way.
35 Indophenol samples were eluted from SPE cartridges in 2 mL methanol. Samples were placed in a
36 bench-top centrifuge for 2 minutes at 20 000xG to remove particulate material derived from the SPE
37 column. A 500 μL sub-sample was used for HPLC purification and GCMS analysis and the remaining 1.5
38 mL was stored at -20°C for any subsequent repetition of the analysis. 500 μL sub-samples were
39 evaporated under oxygen-free nitrogen (OFN) to 200 μL for HPLC, during which it was essential that
40 samples were not reduced to dryness. 175 μL of the 200 μL samples were purified by HPLC using the
41 preparative system, mobile phases and profile described in Clark et al. (2006) in combination with a

1 Gemini-NX 5u C18 110A 250 x 4.6 mm column (Phenomenex, UK) with sample peak collection at a
2 retention time of 38-40 minutes. Collected sample fractions were blown dry under OFN at room
3 temperature. Dried samples were stored for > 24 hours over anhydrous silica gel at room temperature
4 prior to GCMS analysis. Samples were derivitised in 50 µL of 2.5 % Sylon HT in n-hexane and incubated
5 at 50 °C for 4 hours. Samples were analysed by GCMS using the system, ramping profiles and extracted
6 ions described in Clark et al. (2006). Internal standards were used to quantify sample NH_4^+
7 concentration, and when combined with sample enrichment, the rate of NH_4^+ regeneration was
8 determined by applying the Blackburn-Caperon model (Blackburn, 1979; Caperon et al., 1979).

9 SPE columns loaded with sudan-1 samples were brought to room temperature and processed for
10 HPLC purification and GCMS analysis in the following way. Sudan-1 samples were eluted from SPE
11 cartridges in 2 mL of ethyl acetate. 100-300 µL sub-samples were used for further processing while the
12 remaining samples were stored at -20 °C and available for subsequent repeated analysis. 100-300 µL
13 sub-samples were blown dry under OFN, re-dissolved in 200 µL methanol and centrifuged in a bench-
14 top unit at 20 000xG for 2 minutes to remove particulate material derived from the SPE packing.
15 Samples were transferred to GC vials and purified by HPLC. The HPLC system described in Clark et al.
16 (2007) was used in combination with the Gemini column identified above and the mobile phase profile
17 described in Clark et al. (2014). Sample fractions, which were collected at retention time 25.5-27.5
18 minutes, were dried using a Zymark Turbovap evaporation unit at 50 °C using OFN. Dried samples were
19 transferred to GC vials and stored over anhydrous silica gel for 24 hours prior to derivitisation in a 50 µL
20 volume of 2.5 % MTBSTFA in ethyl acetate at 70 °C for 2 hours. The GCMS unit, ramping profile and
21 extracted ions described in Clark et al. (2007) were used to derive sample $\text{NO}_2^-/\text{NO}_3^-$ concentration and
22 isotopic enrichment. The rate of NH_4^+ or NO_2^- oxidation was derived by re-arranging the mixing model of
23 Sweeney et al. (1978) as described in Clark et al. (2007) and by applying the Blackburn-Caperon model
24 (Blackburn, 1979; Caperon et al., 1979).

25 26 2.2 Nitrogen assimilation measurements and the f-ratio.

27 Using 6 L of seawater, nitrogen assimilation rates were derived using ^{15}N techniques. Triplicate
28 660 mL volumes of seawater were separately amended with $^{15}\text{NH}_4^+$ and $^{15}\text{NO}_3^-$ at an enrichment of
29 $7.8\pm 1.8\%$ and $8.0\pm 1.7\%$ of the ambient concentration respectively. Bottles were placed in deck
30 incubators in conditions of simulated in-situ light and temperature. A volume of un-amended seawater
31 was filtered through GF/F and used to derive the ^{15}N natural abundance in particulate matter. Deck
32 incubations were terminated by filtration onto GF/F filters, which were frozen at -20 °C until isotope
33 ratio mass spectrometry analysis was undertaken at the land based laboratory. The rates of nitrogen
34 assimilation (ρNH_4^+ , ρNO_3^-) were determined using the equations of Dugdale and Goering (1967),
35 corrected for nitrogen regeneration using the equations of Kanda et al. (1987).

36 Nitrogen assimilation data (not corrected for isotope dilution) was used to derive f-ratio values by
37 the original formulation as;

$$f - ratio = \frac{\rho\text{NO}_3^-}{\rho\text{NO}_3^- + \rho\text{NH}_4^+}$$

38 The f-ratio was re-calculated using nitrogen assimilation rate data corrected for isotope dilution (f_c -
39 ratio). An additional formulation ($f_{\text{regen-ratio}}$) calculated the f-ratio by including a consideration of

1 previously regenerated NO_3^- within P_1 , represented as the fraction of the total NO_3^- pool remaining as
2 new NO_3^- (R_{NO_3});

$$f_{\text{regen} - \text{ratio}} = \frac{(\rho\text{NO}_3^- \cdot R_{\text{NO}_3})}{((\rho\text{NO}_3^- \cdot R_{\text{NO}_3}) + \rho\text{NH}_4^+)}$$

3 The term R_{NO_3} was calculated using the following procedure and assumptions; it was assumed that
4 R_{NO_3} was conserved (i.e. no mixing took place); that NO_3^- assimilation was restricted to a 12 hour light
5 phase; that phytoplankton did not differentiate between 'new' and 'regenerated' NO_3^- ; that the
6 measured rate of NO_2^- oxidation (which regenerates NO_3^-) was sustained for each 24 hour iteration. As
7 an indication of the utility of using NO_3^- assimilation and regeneration processes to reflect NO_3^- pool
8 turnover, a variance of up to $\pm 25\%$ in calculated compared to measured NO_3^- pool concentration was
9 measured on a daily basis. However, over the duration of the study (T_{-1} - T_7) this difference was -0.2% ,
10 indicating that changes in ambient NO_3^- concentration was adequately described by considering only
11 these processes within the constraints stated.

12 Using T_{-1} as an example, the ambient pool was assumed to have a R_{NO_3} value of 1, indicating that it
13 was composed of 'new' NO_3^- only. The amount of NO_3^- regenerated in this 24 h period was calculated
14 and added to the ambient concentration. The value of R_{NO_3} after this 24 hour period was calculated by
15 dividing the ambient pool concentration (all new NO_3^- for this first time point) by the sum of ambient
16 and regenerated NO_3^- to give a value of 0.94. For the next 24 hour period (T_0), the concentration of
17 'new' NO_3^- was calculated by multiplying the T_0 ambient NO_3^- concentration by the T_{-1} R_{NO_3} value. The
18 R_{NO_3} value at the end of this 24 hour period was calculated by dividing the concentration of new NO_3^- by
19 the sum of ambient and newly regenerated (i.e. within T_0) NO_3^- to provide a value of 0.81. This process
20 was repeated for the study period.

21

22 2.3 Primary productivity measurements

23 Phytoplankton productivity was measured using the ^{14}C method (Tilstone et al., 2009). Samples were
24 collected pre-dawn from 5 depths (97%, 55%, 33%, 14%, 1% sPAR). Triplicate 75 mL subsamples were
25 amended with between 185 and 740 kBq (5–20 μCi) $\text{NaH}^{14}\text{CO}_3$ and incubated on-deck for 24 hours at
26 simulated sPAR depth. Incubations were terminated by sequential filtration through 2 μm and 0.2 μm
27 polycarbonate filters. ^{14}C disintegration was measured on-board using a TriCarb liquid scintillation
28 counter.

29

30 2.4 Chlorophyll concentration

31 Chlorophyll 'a' samples were collected simultaneously with seawater used for primary productivity
32 measurements; 250mL subsamples were collected from 5 depths (97%, 55%, 33%, 14%, 1% sPAR) from
33 pre-dawn CTD casts and immediately filtered sequentially through a 2 μm and 0.2 μm polycarbonate
34 filters. Filters were soaked in 10mL 90% acetone for 12 hours and extracts analysed fluorometrically
35 using a Trilogy Turner fluorometer calibrated against pure chlorophyll 'a' standards (Sigma).

36

37 2.5 Microscopy

38 Seawater samples were collected from 5 depths (97%, 55%, 33%, 14%, 1% sPAR) during pre-dawn
39 CTD casts. Samples were immediately fixed in acid-Lugol's iodine solution (2% final concentration).

1 Where possible cells were identified to species-level according to the published literature and assigned
2 to three functional groups (diatoms (centric & pennate), dinoflagellates, flagellates). Cells were
3 enumerated and expressed as cells·mL⁻¹.

4 5 2.6 Inorganic nutrients

6 Seawater samples were collected from a range of depths during pre-dawn CTD casts into cleaned,
7 acid-washed, and 'aged' high density polyethylene sample bottles, using clean handling and analysis
8 procedures. Samples were analyzed immediately. Nitrate, nitrite, ammonium, phosphate and silicate
9 were measured colorimetrically with a 5-channel segmented flow Bran and Luebbe AAIII autoanalyzer,
10 using methods described previously (Woodward and Rees, 2001).

11 12 3. Results and discussion

13 The inert dual tracers SF₆ and ³He (Nightingale et al., 2000) in combination with drifter buoys were
14 used in this study so that filament progression and biological community development could be
15 followed in Lagrangian mode as the water mass advected offshore (Fig. 1). The loss of tracers to the
16 atmosphere, their dilution due to mixing with unlabelled water and the detection limit of GC analysis
17 constrained patch monitoring duration. A detailed description of filament dynamics forming off Cap
18 Blanc during this study is presented in Meunier et al. (2012). Both North and South Atlantic Central
19 Water (NACW and SACW respectively) is upwelled in this region and the contribution to filaments from
20 each source can be distinguished; SACW generally contains higher nutrient concentrations and has
21 higher temperature with lower oxygen and salinity. Optimum parameter analysis (Rees et al., 2011)
22 demonstrated that the filament studied was dominated by NACW (50-80%).

23 P₁ was identified using a combination of near-real time remotely sensed data and water column
24 profiling. Following identification, observational measurements were undertaken and SF₆/³He tracers
25 were deployed at a depth of 5m in a square spiral (1.0 x 0.8km) around a central drifting buoy. Tracers
26 were detected throughout the surface Mixed Layer Depth (MLD) of 50 m within 1 day of deployment.
27 Extensive mapping exercises were conducted to describe P₁'s progression as the water mass advected
28 offshore in a south-westerly then westerly direction. Mapping enabled the patch centre to be located
29 for daily observational measurements. During this study, P₁ remained tightly constrained for the first 3
30 days until the patch left the continental shelf area and entered the upper slope and shelf break regions.
31 During this latter stage enhanced vertical mixing due to increased water column depth combined with
32 horizontal shear associated with patch proximity to the northern edge of the filament lead to P₁
33 elongation and dispersion.

34 35 3.1 Description of the physical and chemical regime.

36 Selected chemical, biological and physical characteristics of the water column are presented in Fig.
37 1-4. As P₁ advected offshore its temperature increased from ≈ 16.4 °C on T₋₁ to >17.6 °C by T₇ (Fig 1).
38 Profiles of water column temperature demonstrated changes in vertical structure as the mixed layer
39 depth increased from approximately 50m (T₋₁ – T₂) to 100m coinciding with the continental shelf to shelf
40 break transition (T₃, Loucaides et al., 2012). Nutrient concentrations in P₁ were greatest during the first
41 day of Lagrangian study and then progressively decreased (with the exception of NO₂⁻; Fig. 2). On

1 average, NO_3^- concentration decreased from $9.0 \pm 0.1 \mu\text{mol}\cdot\text{L}^{-1}$ to $4.6 \pm 0.3 \mu\text{mol}\cdot\text{L}^{-1}$, Si concentration
2 decreased from $2.7 \pm 0.1 \mu\text{mol}\cdot\text{L}^{-1}$ to $0.9 \pm 0.1 \mu\text{mol}\cdot\text{L}^{-1}$ and PO_4^{3-} concentration decreased from 0.7 ± 0.1
3 $\mu\text{mol}\cdot\text{L}^{-1}$ to $0.4 \pm 0.1 \mu\text{mol}\cdot\text{L}^{-1}$. The greatest decrease in nutrient concentrations occurred on the
4 continental shelf. Following advection over the shelf break, these nutrient concentrations continued to
5 decrease albeit at a lower rate. By contrast, NO_2^- concentration remained relatively stable for the
6 duration of the study at $0.31 \pm 0.05 \mu\text{mol}\cdot\text{L}^{-1}$ while a simple increasing or decreasing trend in NH_4^+
7 concentration was not evident; an average value of $0.8 \pm 0.23 \mu\text{mol}\cdot\text{L}^{-1}$ was measured.

8 Nutrient stoichiometry of the upwelled P_1 water mass (i.e. within the upper mixed layer) indicated
9 nitrogen deficiency (Fig. 3); regression provided a N:P value of 13.9:1 compared to a value of 17.7:1
10 below the mixed layer (incorporating depths up to 1400 m). This value for the photic zone is consistent
11 with the range of 10-16 reported for freshly upwelled coastal waters by Zindler et al. (2012) in their
12 study of the Mauritanian upwelling. The difference in N:P values between depths i.e. for P_1 within the
13 upper mixed layer compared to depths below this, is likely to reflect the relatively rapid biological
14 consumption of N relative to P within the photic zone (Zindler et al., 2012). In contrast, the Namibian
15 shelf's mud belt is a region of continuous N loss and P efflux to the pelagic environment of the Benguela
16 upwelling system, leading to characteristically low N:P ratios. Gregor and Monteiro (2013), who
17 reported pelagic N:P values of 7.2-12.3, identified denitrification and sulphate reduction as anoxic
18 benthic processes leading to this relative nitrogen deficiency, supported by Flohr et al. (2014).

19 The relative nitrogen deficiency measured in P_1 implied a relative P-excess (P^* , calculated as $[\text{PO}_4^{3-}] -$
20 $([\text{NO}_3^-]/16)$). An average P^* of $72 \pm 18 \text{ nmol}\cdot\text{L}^{-1}$ (Fig. 2f and 3) indicated that P_1 exported phosphate to the
21 adjacent oligotrophic gyre of the North Atlantic. The magnitude of this export was less than the value of
22 $< 300 \text{ nmol}\cdot\text{L}^{-1}$ reported for phosphate advection to the South Atlantic gyre by the Benguela Upwelling
23 System (Flohr et al., 2014). A P^* decline towards zero would be anticipated with offshore advection due
24 to nitrogen fixation, supported by atmospheric dust associated iron inputs to the North Atlantic derived
25 from the Sahara region. Dust inputs mitigate the enhanced iron requirements of nitrogen fixing
26 diazotrophs (Moore et al. 2009), ultimately providing a new nitrogen source to the North Atlantic Ocean
27 (Deutsch et al., 2007). In their study of the Benguela Upwelling region, Sohm et al. (2011) suggested that
28 environmental conditions influencing nitrogen fixation are poorly understood and that nitrogen fixing
29 activity extends beyond the tropical and sub-tropical low nutrient regions characteristically considered,
30 to include cool, high nutrient regions. They reported nitrogen fixation rates approaching $8 \text{ nmol}\cdot\text{L}^{-1}\cdot\text{d}^{-1}$,
31 potentially supported by sedimentary sources of iron during a period of low atmospheric dust input. In
32 contrast, undetectable or low rates of nitrogen fixation ($< 1 \text{ nmol}\cdot\text{L}^{-1}\cdot\text{d}^{-1}$) in the Benguela have been
33 reported to make an insignificant contribution to new production (Staal et al., 2007; Benavides et al.,
34 2014; Wasmund et al., 2015). A comparable conclusion for freshly upwelled water was reached during
35 the present study as nitrogen fixation rates in P_1 were undetectable (Rees, unpubl).

36 Analysis demonstrated that nutrient drawdown during P_1 progression was driven by biological
37 processes (Loucaides et al., 2012); factors such as horizontal and vertical mixing with low nutrient water
38 masses derived from outside of the upwelled filament were unlikely to have made a significant
39 contribution. However, an entrainment event associated with increased mixed layer depth lead to a
40 small but measurable recovery in nutrient concentrations during T_3 - T_4 .

1 Nutrient drawdown supported high rates of primary production (Fig. 4). Rates were measured within
2 the range $0.1\text{-}0.7 \text{ molC}\cdot\text{m}^{-2}\cdot\text{d}^{-1}$ which sets an upper limit for C-export through a combination of
3 particulate material sedimentation (Nowald et al., 2015), lateral transport of dissolved organic matter
4 (Álvarez-Salgado et al., 2007), and trophic transfer. The range in primary productivity was comparable to
5 the value of $0.2 \text{ molC}\cdot\text{m}^{-2}\cdot\text{d}^{-1}$ reported for the region by Minas et al. (1986) and potentially exceeds that
6 measured in other upwelling areas; values of $0.02\text{-}0.21 \text{ molC}\cdot\text{m}^{-2}\cdot\text{d}^{-1}$ were reported for the Iberian
7 upwelling (Joint et al., 2001a; Álvarez-Salgado et al., 2002; Arístegui et al., 2006), $0.01\text{-}0.46 \text{ molC}\cdot\text{m}^{-2}\cdot\text{d}^{-1}$
8 were reported for the Peruvian upwelling (Fernández et al., 2009), an average of $0.23 \text{ molC}\cdot\text{m}^{-2}\cdot\text{d}^{-1}$ was
9 reported for the Southern Benguela (Shannon and Field, 1985) and $0.07 \text{ molC}\cdot\text{m}^{-2}\cdot\text{d}^{-1}$ was reported for
10 the Californian Upwelling Ecosystem (Santoro et al., 2010).

11 In terms of distribution, the highest rates of primary productivity were associated with the
12 continental shelf region ($0.49\text{-}0.69 \text{ molC}\cdot\text{m}^{-2}\cdot\text{d}^{-1}$), with rates decreasing as P_1 advected over the shelf
13 break ($0.11\text{-}0.25 \text{ molC}\cdot\text{m}^{-2}\cdot\text{d}^{-1}$). This distribution was characteristic of the coastal North West African
14 region, with high biological productivity associated with the continental shelf area influenced by
15 upwelling (Mittelstaedt, 1991; Arístegui et al., 2009).

16 3.2 Phytoplankton composition and nitrogen assimilation.

17 Freshly upwelled water is extremely low in chlorophyll content and productivity, and would
18 characteristically contain a NO_3^- concentration in the range $9\text{-}15 \mu\text{mol}\cdot\text{L}^{-1}$ for this region (Arístegui et al.,
19 2009, noting that P_1 's composition of NACW and SACW would place freshly upwelled water towards the
20 upper end of this range). Consequently, productivity had become established and decreased NO_3^- by up
21 to $6 \mu\text{mol}\cdot\text{L}^{-1}$ prior to this study which followed the removal of a further $4 \mu\text{mol}\cdot\text{L}^{-1}$ of NO_3^- . During P_1
22 progression, clear transitions in phytoplankton abundance, nitrogen biomass and nitrogen assimilation
23 activity took place (Fig. 5). The highest abundance of all phytoplankton was measured during the first 3
24 days of Lagrangian study ($T_0\text{-}T_2$). Although flagellates were numerically dominant, diatoms dominated
25 carbon biomass representing between 40-80% (data not shown). Cell abundance decreased beyond T_2
26 although specific phytoplankton classes represented a consistent proportion of total abundance
27 suggesting that selective removal was not an important factor; for the duration of this study, diatoms
28 represented $12.7\pm 5.7\%$, dinoflagellates represented $0.10\pm 0.02\%$, flagellates represented $87.2\pm 5.7\%$ of
29 total cell abundance. The trend of progressively diminishing phytoplankton abundance was reflected in
30 the concentration of PON which decreased by 75% within 8 days.

31 During this study, NH_4^+ assimilation was measured within the range $6.1\text{-}32.8 \text{ nmol}\cdot\text{L}^{-1}\cdot\text{h}^{-1}$, while NO_3^-
32 assimilation was measured within the range $3.9\text{-}43.8 \text{ nmol}\cdot\text{L}^{-1}\cdot\text{h}^{-1}$. There are relatively few studies of
33 nitrogen assimilation in the North West African region against which to draw comparisons; NO_3^-
34 assimilation measured within the photic zone was previously reported in the range $<0.2\text{-}31 \text{ nmol}\cdot\text{L}^{-1}\cdot\text{h}^{-1}$
35 (Varela et al., 2005; Dugdale et al., 1990) while NH_4^+ assimilation was reported in the range $<0.2\text{-}105$
36 $\text{ nmol}\cdot\text{L}^{-1}\cdot\text{h}^{-1}$ (Varela et al., 2005; Benavides et al., 2013). The fact that rates of NH_4^+ and NO_3^- assimilation
37 were broadly similar for P_1 , despite the difference in nitrogen source availability was perhaps the most
38 striking observation. The average P_1 NH_4^+ and NO_3^- concentrations were $0.80\pm 0.23 \mu\text{mol}\cdot\text{L}^{-1}$ and
39 $6.22\pm 1.20 \mu\text{mol}\cdot\text{L}^{-1}$ respectively, differing by almost one order of magnitude. Results underscore the
40 importance of regenerated nitrogen in supporting phytoplankton nitrogen requirements even from the
41

1 early stages of upwelling and imply that this form of inorganic nitrogen was rapidly recycled. The
2 significance of nitrogen regeneration in upwelling regions has previously been highlighted (Raimbault
3 and Garcia, 2008; Clark et al., 2011; Fernández and Farías, 2012; Benavides et al., 2014).

4 Within the conveyor belt scheme describing productivity cycles in upwelling systems (Wilkerson and
5 Dugdale, 2008), the increase of phytoplankton growth in response to favourable light and nutrient
6 conditions (shift-up phase) is followed by a shift-down phase driven by factors such as sedimentation
7 and grazing. Cycles last between five and seven days. The trend of progressively diminishing indicators
8 of phytoplankton abundance and activity in combination with a calculated residence time within the
9 photic zone of 3 days for upwelled water prior to T_0 (Meunier et al., 2012; Loucaides et al., 2012)
10 suggested that the peak and shift-down stages of phytoplankton productivity were investigated here.
11 Contributory factors (excluding sedimentation and grazing for which we have no data) to the shift-down
12 phase are discussed below.

13 In previous studies of upwelling regimes, inorganic nutrient availability has been identified as a
14 limiting resource driving changes in community structure and productivity (Wilkerson and Dugdale,
15 2008). Nutrient limitation of larger cells, which dominated productivity in the present study, may have
16 been a contributory factor. For example, the average N:Si ratio for the duration of P_1 (4.49 ± 0.78)
17 indicated potential silicate limitation of diatom growth (Brzezinski, 1985; Gilpin et al., 2004). However,
18 relatively high nutrient concentrations were detected by T_7 and a shift in community structure was not
19 observed; the comparable decrease in cell abundance across all phytoplankton classes implied a less
20 specific driver behind the decrease in biomass during the relatively short duration of this investigation.

21 Light may be considered as a limiting resource; profiles of light intensity and optical depth diminish
22 during the prolific growth of phytoplankton in surface waters; average daily light exposure for cells will
23 also diminish during water column structure transitions as observed beyond T_2 where MLD exceeded
24 the 1% sPAR depth. Under these circumstances, light limitation would be expressed as a preferential use
25 of NH_4^+ over NO_3^- due to the differential energetic demands (Clark et al., 2002; Flynn et al., 2002). This
26 was not observed during T_{-1} - T_2 . However, NH_4^+ assimilation rate consistently exceeded NO_3^- assimilation
27 beyond T_3 (the point at which MLD exceeded the 1% sPAR depth), potentially supporting this
28 mechanism to describe a characteristic feature of nitrogen assimilation by phytoplankton in upwelled
29 water (Dickson and Wheeler, 1995; Kudela et al., 1997) and contributing to the progressive decrease in
30 indicators of phytoplankton activity and biomass.

31 32 3.3 The regeneration of inorganic nitrogen.

33 Evidence presented here demonstrated that the regeneration of inorganic nitrogen sustained
34 phytoplankton productivity during P_1 development. Nutrient regeneration is a product of heterotrophic
35 DOM degradation by microplankton (bacteria, flagellates, ciliates), following its release from
36 phytoplankton due to grazing (Probyn, 1987; Varela et al., 2003; Bode et al., 2004) or its active release
37 from phytoplankton during nutrient assimilation (Bronk et al., 1994; Raimbault and Garcia, 2008;
38 Benavides et al., 2013). Alternative routes of NH_4^+ regeneration in upwelling systems may be minor (e.g.
39 the activity of zooplankton; Bode et al., 2004; Bronk and Steinberg, 2008; Fernández-Urruzola et al.,
40 2014) or difficult to quantify, such as the contribution from the photochemical degradation of DON
41 (Rain-Franco et al., 2014).

1 During the present study, NH_4^+ was regenerated at rates within the range 9.4-85.0 $\text{nmol}\cdot\text{L}^{-1}\cdot\text{h}^{-1}$ (Fig.
2 6). We are unaware of previous studies for the Mauritanian system with which to compare this data. For
3 Cape Ghir (north of the study location), Benavides et al. (2013) reported NH_4^+ regeneration rates of
4 8 $\text{nmol}\cdot\text{L}^{-1}\cdot\text{h}^{-1}$. For the Benguela system Probyn (1987; 1990) reported rates of 0-125 $\text{nmol}\cdot\text{L}^{-1}\cdot\text{h}^{-1}$ and
5 Benavides et al. (2014) reported rates of 90-130 $\text{nmol}\cdot\text{L}^{-1}\cdot\text{h}^{-1}$. For the less productive Iberian upwelling
6 system rates of 0.09-2.52 $\text{nmol}\cdot\text{L}^{-1}\cdot\text{h}^{-1}$ have been reported (Clark et al., 2011). Benavides et al. (2013)
7 speculated in their study of the Benguela system that high rates of NH_4^+ regeneration were driven by a
8 high abundance of dinoflagellates and mixotrophic microflagellates. In the present study, the highest
9 rate of NH_4^+ regeneration was measured at T_0 , coinciding with the highest ambient ammonium
10 concentration and abundance of phytoplankton, notably flagellates. This offered circumstantial
11 evidence supporting a role for microflagellates in NH_4^+ regeneration (Benavides et al., 2013). Conversely,
12 bacterial abundance derived from analytical flow cytometry (data not shown) did not offer any clear or
13 statistically significant link with measured rates of NH_4^+ regeneration suggesting that this route may
14 have been of minor importance. Considering all data, an NH_4^+ pool turnover of $1.2\pm 0.7\text{ d}^{-1}$ due to
15 regeneration and a ratio of 1.7 ± 1.1 for NH_4^+ regeneration to assimilation rate demonstrated the rapidity
16 of NH_4^+ recycling that was sufficient to meet phytoplankton requirements, as also reported for other
17 upwelling systems (Benavides et al., 2013; 2014; Raimbault and Garcia, 2008; Clark et al., 2011;
18 Fernández and Farías, 2012).

19 A sink for regenerated NH_4^+ is the nitrification process. The sequential oxidation of NH_4^+ to NO_2^- and
20 NO_3^- is known not to be restricted to aphotic depths (Raimbault and Garcia, 2008; Clark et al., 2008;
21 2014) and has been reported in other upwelling systems (Clark et al., 2011; Fernández and Farías, 2012;
22 Benavides et al., 2014). In their study of the Chilean Upwelling system, Fernández and Farías (2012)
23 demonstrated that oxygen concentrations have an important influence over nitrogen cycle processes,
24 influencing the vertical distribution of nitrifying microorganisms. In oxic photic zone conditions
25 comparable to P_1 , these authors suggested that Crenarchaeota rather than bacteria dominate nitrifying
26 activity.

27 During the present study, $20\pm 10\%$ of regenerated NH_4^+ entered the nitrification pathway. Rates of
28 NH_4^+ and NO_2^- oxidation were $0.30\text{-}8.75\text{ nmol}\cdot\text{L}^{-1}\cdot\text{h}^{-1}$ and $25.55\text{-}81.11\text{ nmol}\cdot\text{L}^{-1}\cdot\text{h}^{-1}$ respectively, resulting
29 in an average turnover of $0.3\pm 0.2\text{ d}^{-1}$ and $0.2\pm 0.1\text{ d}^{-1}$ for NO_2^- and NO_3^- respectively. We are unaware of
30 previous nitrification rate measurements for the Mauritanian system and as a general observation such
31 measurements are rare for upwelling systems. For the Benguela system, NO_3^- regeneration rates of 0.6-
32 15.5 $\text{nmol}\cdot\text{L}^{-1}\cdot\text{h}^{-1}$ have been reported (Füssel et al., 2011; Benavides et al., 2014) although in Cape Ghir
33 nitrification was not detected (Benavides et al., 2013). In the Iberian system, Clark et al. (2011) reported
34 rates of $0.06\text{-}3.74\text{ nmol}\cdot\text{L}^{-1}\cdot\text{h}^{-1}$ and $0.04\text{-}24.76\text{ nmol}\cdot\text{L}^{-1}\cdot\text{h}^{-1}$ for NH_4^+ and NO_2^- oxidation respectively.

35 The average coupling ratio ($\text{NH}_4^+:\text{NO}_2^-$ oxidation rate) was 0.11 ± 0.07 , indicating that these processes
36 were substantively uncoupled; NO_2^- oxidation rate exceeded NH_4^+ oxidation rate by several fold as
37 previously reported (Lipschultz et al., 1990; Beman et al., 2010, 2013; Clark et al., 2011, 2014; Füssel et
38 al., 2011; Fernández and Farías, 2012; Ganesh et al., 2015). The extent of decoupling would imply that
39 NO_2^- oxidation was unsustainable, as NO_2^- would be removed within 1 day at the prevailing NO_2^-
40 oxidation rates. However, a NO_2^- concentration of $\approx 0.3\mu\text{mol}\cdot\text{L}^{-1}$ persisted in the photic zone for the
41 duration of the study indicating an approximate balance between NO_2^- production and consumption

1 processes. Füssel et al. (2011) suggested that in suboxic environments associated with the Namibian
2 oxygen minimum zone, NO_2^- produced via NO_3^- reduction (the first stage of denitrification) could, in
3 combination with NH_4^+ oxidation, support the observed rates of NO_2^- oxidation. Such a mechanism
4 would be unlikely for the present study as P_1 oxygen concentrations exceeded $200 \mu\text{mol}\cdot\text{L}^{-1}$ (results not
5 shown), effectively excluding denitrification which is associated with extremely low oxygen or anoxic
6 conditions (Naqvi et al., 2006). We speculate that these observations could be reconciled by a
7 mechanism in which particle bound nitrifying organisms existed in close physical and chemical
8 association. Diverse sources of evidence support this association (Ward, 2008; Ganesh et al., 2015). Via
9 this mechanism the microbially mediated degradation of particulate organic matter within the
10 microenvironment of a recently formed biological particle (Stocher, 2012) would regenerate NH_4^+
11 directly supporting NH_4^+ oxidation; resultant NO_2^- would support NO_2^- oxidation and regenerated NO_3^-
12 would be released from particles. In contrast, neither NH_4^+ nor NO_2^- would be released from particles to
13 an extent that reflected the stoichiometric rate relationships within, or closely associated with the
14 particle (potentially contributing to the persistent budgetary ' NH_4^+ deficit' previously identified in the
15 Iberian upwelling study of Clark et al., 2011). If such a mechanism were to operate, specific tracer
16 methods would underestimate nitrogen regeneration rates (specifically NH_4^+ regeneration and oxidation
17 rates) in ecosystems characteristically enriched in newly formed marine particles. If this were the case,
18 the extent of decoupling would imply that the substantial majority of nitrification within P_1 was
19 associated with particles. It is unlikely that the micro-environment of marine particles reflects that of
20 bulk water (Stocker, 2012), offering a rationale for our inability to establish robust relationships
21 between environmental factors and nitrification rates beyond light inhibition, which has limited model
22 development (Bouskill et al., 2011; Füssel et al., 2011; Smith et al., 2014a). Additionally, should such a
23 mechanism operate, particle bound nitrifying organisms would be alleviated to an extent from direct
24 competition with phytoplankton for NH_4^+ (Smith et al., 2014b).

25

26 3.4 F-ratio formulations.

27 The present study demonstrated that nitrification was measurable from the inception of P_1 implying
28 that the fraction of regenerated NO_3^- progressively increased within days of upwelled water reaching
29 the photic zone. F-ratio formulations for P_1 are presented in Fig. 7 using simultaneously measured rates
30 of nitrogen assimilation and regeneration. Using the original formulation, the highest f-ratio values were
31 derived during the first 3 days of Lagrangian study ($f=0.44-0.63$), generally decreasing as P_1 advected
32 offshore ($f=0.32-0.38$). A study of this region by Minas et al. (1982) provided an f-ratio value of 0.9 but
33 did not consider the role of NH_4^+ regeneration. A revised value of 0.64 was provided by Minas et al.
34 (1986), comparable to that measured during the earliest stages of this study. Correcting f-ratio values
35 for isotope dilution (f_c ratio) made only minor differences. However, accounting for the fraction of
36 regenerated NO_3^- (in addition to isotope dilution; f_{regen} ratio) lead to a cumulative decrease in values
37 relative to the original formulation. Results implied that within ≈ 6 days, the fraction of regenerated NO_3^-
38 was greater than 50% and that the transition from 'new' to a 'regenerated' NO_3^- pool occurred rapidly
39 (i.e. the order of days, not weeks). Given the evidence for nitrification in other upwelling systems (Ward,
40 2005; Fernández et al., 2009; Clark et al., 2011, Benavides et al., 2014), it is likely that NO_3^- based
41 exportable production from such systems has been over-estimated historically.

3.5. Calculating the carbon export of P_1 .

Carbon export supported by new production was estimated using the approach of Eppley and Peterson (1979) as the product of f-ratio and primary production. We compared the original formulation (f-ratio) to alternative formulations; f_c ratios (corrected for isotope dilution) and f_{regen} ratio (corrected for isotope dilution and regenerated NO_3^-).

Rees et al. (2011) estimated that the time taken for P_1 to mature from newly-upwelled to open ocean conditions was approximately 14 days, which we confirmed by extrapolation of integrated primary production rates along an exponential gradient ($\text{PP} = 801.72 e^{-0.253\text{Time}}$, $r^2 = 0.93$). Rates decreased from $0.69 \text{ molC}\cdot\text{m}^{-2}\cdot\text{d}^{-1}$ (T_{-1}) to approximately $0.02 \text{ molC}\cdot\text{m}^{-2}\cdot\text{d}^{-1}$ on day 14, comparable to rates reported for the oligotrophic North East Atlantic (Tilstone et al., 2009). The mean area of P_1 was estimated from surface sea temperature images at $1.29 \times 10^4 \text{ km}^2$ while upwelling activity characteristics were also considered. For the purpose of this estimation we assumed that the persistence of upwelling north of 20°N enabled extrapolation of primary production measured during P_1 over 12 months. By integrating primary production over the 14 day period between maximum upwelling and open-ocean conditions and extrapolating to the mean filament area we estimated annual primary production of 12.38 TgC. The fraction of annual productivity available for export derived using the f-ratio was 6.19 TgC (50%); using the f_c ratio exportable production was 6.01 TgC (49%); using the f_{regen} ratio exportable production was 4.73 TgC (38%). Comparisons with previous estimations are complicated by differences in filament location, geographical area, activity, and integration depth, ranging from $1.12\text{-}2.62 \text{ TgC}\cdot\text{y}^{-1}$ (Helmke et al., 2005) to $3.1 \text{ TgC}\cdot\text{y}^{-1}$ (Álvarez-Salgado et al., 2007), which are of similar order to our f_{regen} ratio estimates. Within the constraints of our assumptions, results suggest that both isotope dilution and the fraction of previously regenerated NO_3^- can be important sources of error for nitrogen based estimations of C-export.

4. Conclusions

For open ocean systems, the limitation to the new production paradigm that NO_3^- is not necessarily 'new' is now well established; to this we add that even within upwelling regions where genuinely new NO_3^- is supplied to the photic zone, the fraction of regenerated NO_3^- increases rapidly. Since the instantaneous ratio of new to regenerated NO_3^- cannot readily be derived this adds uncertainty to f-ratio values. Upwelling zones are unquestionably highly productive. However, our data indicate that nitrification in these waters is significant. It impacts upon f-ratio derived estimations of new production and carbon export by diluting $^{15}\text{NO}_3^-$ tracer and facilitating a transition in NO_3^- pool provenance from a source of new towards a source of regenerated nitrogen.

Acknowledgements

We thank Carol Robinson (chief scientist), Ricardo Torres and Phil Nightingale for cruise leadership and SF_6 mapping, and the officers and crew of the RRS Discovery cruise D338. We thank NEODAAS for providing satellite data to SOLAS-ICON. We thank Lisa Al-Moosawi for isotope ratio mass-spectrometry analysis and two anonymous reviewers for constructive comments during the review process. This study was supported by NERC grant NE/C517176/1 (UK-SOLAS) and by Theme 2 of NERC Oceans 2025.

1
2
3
4
5
6
7
8
9
10
11
12
13
14
15
16
17
18
19
20
21
22
23
24
25
26
27
28
29
30
31
32
33
34
35
36
37
38
39
40
41

References

Álvarez-Salgado, X.A., Beloso, S., Joint, I., Nogueira, E., Chou, L., Perez, F.F., Groom, S., Cabanas, J.M., Rees, A.P. and Elskens, M.: New production of the NW Iberian shelf during the upwelling season over the period 1982–1999, *Deep-Sea Res. Part I*, 49, 1725–1739, doi:10.1016/S0967-0637(02)00094-8, 2002.

Álvarez-Salgado, X. A., Arístegui, J., Barton, E.D. and Hansell, D. A.: Contribution of upwelling filaments to offshore carbon export in the subtropical Northeast Atlantic Ocean. *Limnol. Oceanogr.* 52, 1287-1292, doi:10.4319/lo.2007.52.3.12872007, 2007.

Arístegui, J., Álvarez-Salgado, X.A., Barton, E.D., Figueiras, F.G., Hernández-León, S., Roy, C. and Santos, A.M.P.: Oceanography and fisheries of the Canary Current Iberian region of the Eastern North Atlantic, p. 877–931. In A. Robinson and K. H. Bronk [eds.], *The global coastal ocean: Interdisciplinary regional studies and syntheses*. Harvard Univ. Press, 2006.

Arístegui, J., Barton, E.D., Álvarez-Salgado, X. A., Santos, M. P., Figueiras, F. G., Kifani, S., Hernández-León, S., Mason, E., Machú, E. and Demarcq, H.: Sub-regional ecosystem variability in the Canary Current upwelling, *Prog. Oceanogr.* 83, 33-43, 2009. doi:10.1016/j.pocean.2009.07.031, 2009.

Baker, A.R., Kelly, S.D., Biswa, K.F., Witt, M. and Jickells, T.D.: Atmospheric deposition of nutrients to the Atlantic Ocean, *Geophys. Res. Lett.* 30, 2296, doi:10.1029/2003GL018518, 2003

Beman, J.M., Sachdeva, R. and Fuhrman, J.A.: Population ecology of nitrifying Archaea and bacteria in the Southern California Bight. *Environmental Microbiology.* 12, 1282-1292, doi:10.1111/j.1462-2920.2010.02172.x, 2010.

Beman, J.M., Shih, J.L. and Popp, B.N.: Nitrite oxidation in the upper water column and oxygen minimum zone of the eastern tropical North Pacific Ocean, *Int. Soc. Micro. Ecol.* 7, 2192-2205, doi:10.1038/ismej.2013.96, 2013.

Benavides M., Arístegui, J., Agawin, N.S.R., Álvarez-Salgado, X.A., Álvarez, M., and Troupin, C.: Low contribution of N₂ fixation to new production and excess nitrogen in the subtropical northeast Atlantic margin, *Deep-Sea Res., I*, 81, 36-48, doi:10.1016/j.dsr.2013.07.004, 2013.

Benavides M., Santana-Falcón Y., Wasmund, N. and Arístegui, J.: Microbial uptake and regeneration of inorganic nitrogen off the coastal Namibian upwelling system. *J. Mar. Sys.* 140, 123-129, doi:10.1016/j.jmarsys.2014.05.002, 2014.

Blackburn, T.H.: Method for measuring rates of NH₄⁺ turnover in anoxic marine sediments, using ¹⁵N-NH₄⁺ dilution technique, *Appl. Environ. Microbiol.* 37, 760–765, 1979.

1
2 Bode, A., Barquero, S., Gonzalez, N., Alvarez-Ossorio, M. T., and Varela, M.: Contribution
3 of heterotrophic plankton to nitrogen regeneration in the upwelling ecosystem of A Coruña (NW
4 Spain), *J. Plankton Res.* 26, 11–28, doi:10.1093/plankt/fbh003, 2004.
5
6 Bouskill, N.J., Eveillard, D., Chien, D., Jayakumar, A. and Ward, B.B: Environmental factors determining
7 ammonia-oxidizing organism distribution and diversity in marine environments, *Env. Microbiol*, 14, 714-
8 729, doi:10.1111/j.1462-2920.2011.02623.x, 2011.
9
10 Bronk, D.A. and Glibert, P.M.: Contrasting patterns of dissolved organic nitrogen release by two size
11 fractions of estuarine plankton during a period of rapid NH_4^+ consumption and NO_2^- production, *Mar.*
12 *Ecol. Prog. Ser.* 96, 291-299, 1993.
13
14 Bronk, D.A. and Ward, B.B.: Gross and net nitrogen uptake and DON release in the euphotic zone of
15 Monterrey Bay, California, *Limnol. Oceanogr.* 44, 573-585, 1999.
16
17 Bronk, D.A. and Steinberg, D.K.: Nitrogen regeneration. In: *Nitrogen in the Marine Environment*, Capone,
18 D., Bronk, D.A., Mulholland, M.R., Carpenter, E.J. (eds). Elsevier Press, pp 385-467, 2008.
19
20 Bronk, D.A., Glibert, P.M. and Ward, B.B.: Nitrogen uptake, dissolved organic nitrogen release, and new
21 production, *Science*, 265:1843, doi:10.1126/science.265.5180.1843, 1994.
22
23 Brzezinski, M. A.: The Si-C-N ratio of marine diatoms—Interspecific variability and the effect
24 of some environmental variables. *J. Phycol.* 21, 347–357, doi:10.1111/j.0022-3646.1985.00347.x, 1985.
25
26 Caperon, J., Schell, D., Hirota, J. and Laws, E: Ammonium excretion rates in Kaneohe Bay, Hawaii,
27 measured by a ^{15}N isotope dilution technique, *Mar. Biol.* 54, 33–40, doi:10.1007/BF00387049, 1979.
28
29 Chavez, F. and Messié, M.: A comparison of Eastern Boundary Upwelling Ecosystems, *Prog. Oceanogr.* 83,
30 80-96, doi:10.1016/j.jpocean.2009.07.32, 2009.
31
32 Clark, D.R., Flynn, K.J. and Owens, N.J.P.: The large capacity for dark nitrate-assimilation in diatoms may
33 overcome nitrate limitation of growth, *New Phytologist*, doi:10.1046/j.1469-8137.2002.00435.x, 155:
34 101–108, 2002.
35
36 Clark, D.R., Fileman, T.W. and Joint, I.: Determination of ammonium regeneration rates in the
37 oligotrophic ocean by gas chromatography/mass spectrometry, *Mar. Chem.* 98, 121-130,
38 doi:10.1016/j.marchem.2005.08.006, 2006.
39

- 1 Clark, D.R., Rees, A.P. and Joint, I.: A method for the determination of nitrification rates in oligotrophic
2 marine seawater by gas chromatography/mass spectrometry, *Mar. Chem.* 103: 84-96,
3 doi:10.1016/j.marchem.2006.06.005, 2007.
4
- 5 Clark, D.R., Rees, A.P. and Joint, I.: Ammonium regeneration and nitrification rates in the oligotrophic
6 Atlantic Ocean: Implications for new production estimates, *Limnol. Oceanogr.* 53: 52–62,
7 doi:10.4319/lo.2008.53.1.0052, 2008.
8
- 9 Clark, D.R., Miller, P.I., Woodward, E.M.S. and Rees, A.P.: Inorganic nitrogen assimilation and
10 regeneration in the coastal upwelling region of the Iberian Peninsula, *Limnol. Oceanogr.* 56, 1689–1702,
11 doi:10.4319/lo.2011.56.5.1689, 2011.
12
- 13 Clark, D.R., Brown, I.J., Rees, A.P., Somerfield, P.J. and P. I. Miller.: The influence of ocean acidification
14 on nitrogen regeneration and nitrous oxide production in the northwest European shelf sea,
15 *Biogeosciences*, 11, 4985-5005, doi:10.5194/bg-11-4985-2014, 2014.
16
- 17 D’Asaro, E.A.: Lagrangian trajectories on the Oregon shelf during upwelling, *Cont. Shelf Res.*, 24(13–14),
18 1421–1436, doi:10.1016/j.csr.2004.06.003, 2004.
19
- 20 Dickson, M.L. and Wheeler, P.A.: Nitrate uptake rates in a coastal upwelling regime – A comparison of
21 PN-specific, absolute and chl a-specific rates, *Limnol. Oceanogr.* doi:10.4319/lo.1995.40.3.0533, 40, 533-
22 543, 1995.
23
- 24 Deutsch, C., Sarmiento, J.L., Sigman, D.M., Gruber, N. and Dunne, J.P.: Spatial coupling of nitrogen inputs
25 and losses in the ocean, *Nature*, 445, 163-167, doi:10.1038/nature05392, 2007.
26
- 27 Dugdale, R.C., and Goering, J.J.: Uptake of new and regenerated forms of nitrogen in primary
28 productivity, *Limnol. Oceanogr.* 12, 196–206, doi:10.4319/lo.1967.12.2.0196, 1967.
29
- 30 Dugdale, R.C., Wilkerson, F.P. and Morel, A.: Realization of new production in coastal upwelling areas: A
31 means to compare relative performance, *Limnol. Oceanogr.* 35, 822–829,
32 doi:10.4319/lo.1990.35.4.0822, 1990.
33
- 34 Eppley, R.W. and Peterson, B.J.: Particulate organic matter flux and planktonic new production in the
35 deep ocean, *Nature*, 282, 677–680, doi:10.1038/282677a0, 1979.
36
- 37 Fernández, C. and Farías, L.: Assimilation and regeneration of inorganic nitrogen in a coastal upwelling
38 system: ammonium and nitrate utilisation, *Mar. Ecol. Prog. Ser.* 451:1-14, doi:10.3354/meps09683,
39 2012.
40

1 Fernández, C., Raimbault, P., Garcia, N. and Rimmelin, P.: An estimation of annual new production and
2 carbon fluxes in the northeast Atlantic Ocean during 2001, *J. Geophys. Res.*, 110, C07S13,
3 doi:10.1029/2004JC002616, 2005.
4

5 Fernández, C., Farías, L. and Alcaman, M.E.: Primary production and nitrogen regeneration processes in
6 surface waters of the Peruvian upwelling system, *Prog. Oceanogr.* 83, 159–168,
7 doi:10.1016/j.pocean.2009.07.010, 2009.
8

9 Fernández-Urruzola, I., Osma, N., Packard, T.T., Gómez, M. and Postel, L.: Distribution of zooplankton
10 biomass and potential metabolic activities across the northern Benguela upwelling system, *Journal of*
11 *Marine Systems*. 140: 138-149, doi:10.1016/j.jmarsys.2014.05.009, 2014.
12

13 Flohr, A., van der Plas, A.K., Emeis, K.-C., Mohrholz, V. and Rixen, T.: Spatio-temporal patterns of C:N:P
14 ratios in the northern Benguela upwelling system, *Biogeosciences*, 11, 885-897, doi:10.5194/bg-11-885-
15 2014, 2014.
16

17 Flynn, K.J., Clark, D.R. and Owens, N.J.P.: Modelling suggests that optimization of dark
18 nitrogen-assimilation need not be a critical selective feature in phytoplankton, doi:10.1046/j.1469-
19 8137.2002.00436.x, *New Phytologist* 155: 109–119, 2002.
20

21 Füssel, J., Lam, P., Lavik, G., Jensen, M.M., Holtappels, M., Günter, M. and Kuypers, M.M.M.: Nitrite
22 oxidation in the Namibian oxygen minimum zone, *ISME Journal* 1-10, doi:10.1038/ismej.2011.178, 2011.
23

24 Ganesh, S. Bristow, L.A., Larsen, M., Sarode, N., Thamdrup, B. and Stewart, F.J.: Size-fraction partitioning
25 of community gene transcription and nitrogen metabolism in a marine oxygen minimum zone, *ISME*, 9,
26 2682–2696, doi:10.1038/ismej.2015.44, 2015.
27

28 Gilpin, L.C., Davidson, K. and Robertsb, E.: The influence of changes in nitrogen: silicon ratios on
29 diatom growth dynamics, *J. Sea Res.* 51, 21-35, doi:10.1016/j.seares.2003.05.005, 2004.
30

31 Glibert, P.M., Lipshultz, F., McCarthy, J.J. and Altabet, M.A.: Isotope dilution models of
32 uptake and remineralization of ammonium by marine plankton, *Limnol. Oceanogr.* 27, 639–650,
33 doi:10.4319/lo.1982.27.4.0639, 1982.
34

35 Gregor, L. and Monteiro, P.M.S.: Seasonal cycle of N:P:TA stoichiometry as a modulator of CO₂ buffering
36 in eastern boundary upwelling systems, *Geophys. Res. Lett.* 40, 5429-5434, doi:10.1002/2013GL058036,
37 2013
38

39 Helmke, P., Romero, O. and Fischer, G.: Northwest African upwelling and its effect on offshore organic
40 carbon export to the deep sea, *Global Biogeochem. Cyc.* 19, GB4015, doi:10.1029/2004GB002265,
41 2005.

1
2 Intergovernmental Oceanographic Commission, Paris (France), Protocols for the Joint Global Flux Study
3 (JGOFS) core measurements, Manuals Guides 29, 1994.
4
5 Jickells, T. and Moore, C.M.: The importance of atmospheric deposition for ocean productivity, *Annu.*
6 *Rev. Ecol. Evol. Syst.*, 46:481-501, doi:10.1146/annurev-ecolsys-112414-054118, 2015.
7
8 Joint, I., Rees, A.P. and Woodward, E.M.S.: Primary production and nutrient assimilation in the Iberian
9 upwelling in August 1998, *Prog. Oceanogr.* 51, 303–320, doi:10.1016/S0079-6611(01)00072-6, 2001a.
10
11 Joint, I., Inall, M., Torres, R., Figueiras, F.G., Álvarez-Salgado, X.A., Rees, A.P. and Woodward, E.M.S.: Two
12 Lagrangian experiments in the Iberian Upwelling System: Tracking an upwelling event and an offshore
13 filament, *Prog. Oceanogr.*, 51(2–4), 221–248, doi:10.1016/S0079-6611(01)00068-4, 2001b.
14
15 Kanda, J., Laws, E.A., Saino, S.T. and Hattori, A.: An evaluation of isotope dilution effect from
16 conventional data sets of ¹⁵N uptake experiments, *J. Plankton Res.* 19, 79–90,
17 doi:10.1093/plankt/9.1.79, 1987.
18
19 Kudela, R.M., Cochlan, W.P. and Dugdale, R.C.: Carbon and nitrogen uptake response to light by
20 phytoplankton during an upwelling event, *J. Plankton Res.* 19, 609-630, doi:10.1093/plankt/19.5.609,
21 1997.
22
23 Loucaides, S., Tyrrell, T., Achterberg, E.P., Torres, R., Nightingale, P.D., Kitidis, V., Serret, P., Woodward,
24 M. and Robinson, C.: Biological and physical forcing of carbonate chemistry in an upwelling filament off
25 northwest Africa: Results from a Lagrangian study, *Global Biogeochemical Cycles.* 26:GB3008,
26 doi:10.1029/2011GB004216, 2012.
27
28 Lipshultz, F., Wofsy, S.C., Ward, B.B., Codispoti, L.A., Freidrich, G. and Elkins, J.W.: Bacterial
29 transformations of inorganic nitrogen in the oxygen deficient waters of the Eastern Tropical South
30 Pacific Ocean, *Deep Sea Res.* 37, 1513-1541, 1990.
31
32 Martin, A.P. and Pondaven, P.: New production and nitrification in the western subtropical North
33 Atlantic: A modelling study, *Global Biogeochem. Cyc.* 20, GB4014, doi:10.1029/2005GB002608, 2006.
34
35 Meunier, T., Barton, E.D., Barreiro, B. and Torres, R.: Upwelling filaments off Cap Blanc: Interaction of
36 the NW African upwelling current and the Cape Verde frontal zone eddy field? *J. Geophys. Res.* 117,
37 C08031, doi:1029/2012JC007905, 2012.
38
39 Miller, P., Groom, S., McManus, A., Selley, J. and Mironnet, N.: Panorama: A semi-automated AVHRR
40 and CZCS system for observation of coastal and ocean processes, *RSS97: Observations and Interactions,*
41 *Proceedings of the Remote Sensing Society,* 539-544, 1997.

1
2 Minas, T., Packard, T., Minas, M., Coste, B.: An analysis of the production-regeneration system in the
3 coastal upwelling area off N.W. Africa based on oxygen, nitrate and ammonium distribution. *J. Mar. Res.*
4 40, 615-641, 1982.
5
6 Minas, H.J., Minas, M., Packard, T.T.: Productivity in upwelling areas deduced from hydrographic and
7 chemical fields, *Limnol. Oceanogr.* 31(6), 1182-1206, 1986.
8
9 Mitra, A., Flynn, K.J., Burkholder, J.M., Berge, T., Calbet, A., Raven, J.A., Granéli, E., Glibert, P.M., Hansen,
10 P.J., Stoecker, D.K., Thingstad, F., Tillmann, U., Våge, S., Wilken, S. and Zubkov, M.V.: The role of
11 mixotrophic protists in the biological carbon pump, *Biogeosciences*, 11, 995-1005, doi:10.5194/bg-11-
12 995-2014, 2014.
13
14 Mittelstaedt, E.: The ocean boundary along the northwest African coast: Circulation and oceanographic
15 properties at the sea surface, *Prog. Oceanogr.* 26, 307-355, doi:10.1016/0079-6611(91)90011-A, 1991.
16
17 Moore, C.M., Mills, M.M., Achterberg, E.P., Geider, R.J., LaRoche, J., Lucas, M.I., McDonagh, E.L., Pan, X.,
18 Poulton, A.J., Rijkenberg, M.J.A., Suggett, D., Ussher, S.J. and Woodward, E.M.S.: Large-scale distribution
19 of Atlantic nitrogen fixation controlled by iron availability, *Nature Geoscience*, 2, 867-871,
20 doi:10.1038/ngeo667, 2009.
21
22 Moore, C.M., Mills, M.M., Arrigo, K.R., Berman-Frank, I., Bopp, L., Boyd, P.W., Galbraith, E.D., Geider,
23 R.J., Guieu, C., Jaccard, S.L., Jickells, T.D., La Roche, J., Lenton, T.M., Mahowald, N.M., Marañón, E.,
24 Marinov, I., Moore, J.K., Nakatsuka, T., Oschlies, A., Saito, M.A., Thingstad, T.F., Tsuda, A. and Ulloa, O.:
25 Processes and patterns of oceanic nutrient limitation. *Nature Geoscience*, 6, 701-710,
26 doi:10.1038/ngeo1765, 2013.
27
28 Moschonas, G., Gowen, R.J., Stewart, B.M. and Davidson, K.: Nitrogen dynamics in the Irish Sea and
29 adjacent shelf waters: An exploration of dissolved organic nitrogen, *Estuarine, Coastal and Shelf Science*,
30 164, 276-287, doi:10.1016/j.ecss.2015.07.030, 2015.
31
32 Naqvi, S.W.A., Naik, H., Pratihary, A., D'Souza, W., Narvekar, P.V., Jayakumar, D.A., Devol, A.H.,
33 Yoshinari, T. and T. Saino.: Coastal versus open-ocean denitrification in the Arabian Sea, *Biogeosciences*,
34 3, 621-633, doi:10.5194/bg-3-621-2006, 2006.
35
36 Nightingale, P.D., Malin, G., Law, C.S., Watson, A.J., Liss, P.S., Liddicoat, M.I., Boutin, J. and Upstill-
37 Goddard, R.C.: In situ evaluation of air-sea gas exchange parameterizations using novel conservative and
38 volatile tracers, *Global Biogeochem. Cyc.* 14, 373-387, doi:10.1029/1999GB900091, 2000.
39

1 Nowald, N., Iversen, M.H., Fischer, G., Ratmeyer, V., Wefer, G.: Time series of *in-situ* particle properties
2 and sediment trap fluxes in the coastal upwelling filament off Cape Blanc, Mauritania, Prog. Oceanogr.
3 137, 1-11, doi:10.1016/j.pocean.2014.12.015.
4

5 Olson, R.J.: Differential photoinhibition of marine nitrifying bacteria: a possibly mechanisms for the
6 formation of the primary nitrite maximum, J. Mar. Res. 39, 227-238, 1981.
7

8 Pauly, D. and Christensen, V.: Primary production required to sustain global fisheries, Nature, 374(6519),
9 255–257, doi:10.1038/374255a0, 1995.
10

11 Postel, L., Mohrholz, V. and Packard, T.T.: Upwelling and successive ecosystem response in the Northern
12 Benguela Region - an in situ experiment, Journal of Marine Systems 140, 73–81,
13 doi:10.1016/j.jmarsys.2014.07.014, 2014.
14

15 Probyn, T.A.: Ammonium regeneration by microplankton in an upwelling environment, Mar.
16 Ecol. Prog. Ser. 37, 53–64, 1987.
17

18 Probyn, T.A.: Size-fractionated measurements of nitrogen uptake in aged upwelled waters: Implications
19 for pelagic food webs. Limnol. Oceanogr. 35, 202–210, doi:10.4319/lo.1990.35.1.0202, 1990.
20

21 Raimbault, P. and Garcia, N.: Evidence for efficient regenerated production and dinitrogen fixation in
22 nitrogen-deficient waters of the South Pacific Ocean: impact on new and export production estimates,
23 Biogeosciences, 5, 323-338, doi:10.5194/bg-5-323-2008, 2008.
24

25 Rain-Franco, A., Muñoz, C. and Fernández, C.: Ammonium production off central Chile (36°S) by
26 photodegradation of phytoplankton derived and marine dissolved organic matter, PLoSOne, 9, e100224,
27 doi:10.1371/journal.pone.0100224, 2014.
28

29 Rees, A.P., Brown, I.J., Clark, D.R. and Torres, R.: The Lagrangian progression of nitrous oxide within
30 filaments formed in the Mauritanian upwelling, Geophys. Res. Lett. 38, L21606,
31 doi:10.1029/2011GL049322, 2011.
32

33 Santoro, A.E., Casciotti, K.L. and Francis, C.A.: Activity, abundance and diversity of nitrifying archaea and
34 bacteria in the central California Current, Environ. Microbiol. 12, 1989–2006, doi:10.1111/j.1462-
35 2920.2010.02205.x, 2010.
36

37 Shannon, L.V. and Field, J.G.: Are fish stocks food limited in the southern Benguela pelagic ecosystem?
38 Mar. Ecol. Prog. Ser. 22, 7–19, doi:10.3354/meps022007, 1985.
39

1 Smith, J.M., Casciotti, K.L., Chavez, F.P., Francis, C.A.: Differential contribution of archaeal ammonia
2 oxidizer ecotypes to nitrification in coastal surface waters, *ISME*, 8, 1704-1714,
3 doi:10.1038/ismej.2014.11, 2014a.
4

5 Smith, K.M., Chavez, F.P. and Francis, C.A.: Ammonium uptake by phytoplankton regulates nitrification
6 in the sunlit ocean. *PLoS ONE* 9:e108173, doi:10.1371/journal.pone.0108173, 2014b.
7

8 Sohm, J., Hilton, J., Noble, A.E., Zehr, J.P., Saito, M. and Webb, E.A.: Nitrogen fixation in the South
9 Atlantic Gyre and the Benuela Upwelling System, *Geophys. Res. Lett.*, 38, L16608,
10 doi:10.1029/2011GL048315, 2011
11

12 Staal, M.S., Lintel Heckert, S., Brummer, G.J.A., Veldhuis, M., Sikkens, C., Persijn, S. and Stal, L.J.:
13 Nitrogen fixation along north-south transect in the eastern Atlantic ocean, *Limnol. Oceanogr.*, 52, 1305-
14 1316, doi:10.4319/lo.2007.52.4.1305, 2007.
15

16 Stocker, R.: Marine microbes see a sea of gradients, *Science*, 338, 628-633, 2012,
17 doi:10.1126/science.1208929.
18

19 Sweeney, R.E., Liu, K.K. and Kaplan, I.R.: Oceanic nitrogen isotopes and their uses in determining the
20 source of sedimentary nitrogen, *N. Z. Depart. Sci. Ind. Res. Bull.* 220, 9–26, 1978.
21

22 Tilstone, G., Smyth, T., Poulton, A. and Hutson, R.: Measured and remotely sensed estimates of primary
23 production in the Atlantic Ocean from 1998 to 2005, *Deep-Sea Res (II)*, 56, 918-930,
24 doi:10.1016/j.dsr2.2008.10.034, 2009.
25

26 Tomczak, M. and Godfrey, J.S.: *Regional Oceanography: An Introduction* (second ed) Daya, Delhi, India,
27 p. 390, 2003.
28

29 Varela, M.M., Barquero, S., Bode, A., Fernández, E., González, N., Teira, E. and Varela, M.:
30 Microplanktonic regeneration of ammonium and dissolved organic nitrogen in the upwelling area of the
31 NW of Spain: relationships with dissolved organic carbon production and phytoplankton size-structure,
32 *J. Plank. Res.*, 25, 719-736, 2003.
33

34 Varela, M., Bode, A., Fernández, E., Gonzales, N., Kitidis, V., Varela, M., and Woodward, E.M.S.: Nitrogen
35 uptake and dissolved organic nitrogen release in planktonic communities characterized by
36 phytoplankton size structure in the central North Atlantic, *Deep Sea Res. I*, 52, 1637–1661,
37 doi:10.1016/j.dsr.2005.03.007, 2005.
38

39 Wafar, M., L'Helguen, S., Raikar, V., Maguer, J.F., Corre, P.L.: Nitrogen uptake by size-fractionated
40 plankton in permanently well-mixed temperate coastal waters, *J. Plank. Res.* 26, 1207-1218,
41 doi:10.1093/plankt/fbh110, 2004.

1
2
3
4
5
6
7
8
9
10
11
12
13
14
15
16
17
18
19
20
21
22
23
24
25
26
27
28

Ward, B.B.: Temporal variability in nitrification rates and related biogeochemical factors in Monterey Bay, California, USA, *Mar. Ecol. Prog. Ser.* 292, 97-109, doi:10.3354/meps292097, 2005.

Ward, B.: Nitrogen in the Marine Environment, In: *Nitrogen in the Marine Environment*, Capone, D., Bronk, D.A., Mulholland, M.R., Carpenter, E.J. (eds). Elsevier Press, pp 199-261, 2008.

Wasmund, N., Struck, U., Hansen, A., Flohr, A., Nausch, G., Gruttmuller, A., and Voss, M.: Missing nitrogen fixation in the Benguela region, *Deep-Sea Res. I*, 106, 30-41, doi:10.1016/j.dsr.2015.10.007, 2015.

Wilkerson, F. P. and Dugdale, R.C.: The use of large shipboard barrels and drifters to study the effects of coastal upwelling on phytoplankton dynamics, *Limnol. Oceanogr.*, 32(2), 368–382, doi:10.4319/lo.1987.32.2.0368, 1987.

Wilkerson, F.P. and Dugdale, R.C.: Coastal Upwelling, In: *Nitrogen in the Marine Environment*, Capone, D., Bronk, D.A., Mulholland, M.R., Carpenter, E.J. (eds). Elsevier Press, pp 765-801, 2008.

Woodward, E.M.S. and Rees, A.P.: Nutrient distributions in an anticyclonic eddy in the North East Atlantic Ocean, with reference to nanomolar ammonium concentrations, *Deep-Sea Res.* 48, 775–794, doi:10.1016/S0967-0645(00)00097-7, 2001.

Zindler, C., Peeken, I., Marandino, C.A. and Bange, H.W.: Environmental control on the variability of DMS and DMSP in the Mauritanian upwelling region, *Biogeosciences*, 9, 1041–1051, doi:10.5194/bg-9-1041-2012, 2012.

1 **Figure legends**

2 Fig. 1. Panel (a) presents composite sea-surface chlorophyll a (April 20-30th, 2009) of the sampling area.
3 The station locations are identified as white squares. Panel (b) presents the daily lateral SF₆/³He
4 distribution, defined as 40% of the peak concentration. The red line indicates the track of a central
5 marker buoy used in combination with SF₆/³He analysis. Panel (c) presents water column temperature
6 (°C) and includes sampling depths for 55% sPAR (black circles) and 1% sPAR (blue squares). The depth of
7 the upper mixed layer is indicated (red triangles; Loucaides et al., 2012). Note the reversal of dates in
8 panel (c) to aid comparisons between figures.

9
10 Fig. 2. Average concentration of inorganic nutrients within the upper mixed layer; (a) nitrate, (b) nitrite,
11 (c) ammonium, (d) phosphate, (e) silicate. The phosphate excess (P*) is presented in panel (f). Error bars
12 represent one standard deviation for triplicate concentration measurements. Note the reversal of dates
13 to aid comparisons between figures.

14
15 Fig. 3. Ratio between ambient concentrations of nitrate and phosphate. The solid regression line is the
16 Redfield ratio of 16:1. Data from within the surface mixed layer depth (MLD) are presented in panel (a),
17 the regression of which provides a ratio of 13.9:1 and a phosphate excess of 72±18 nmol-P·L⁻¹. Data
18 from below the MLD, presented in panel (b) were collected to a maximum depth of 1.4 km. The
19 regression of this data provided a ratio of 17.7:1.

20
21 Fig 4. Changes in integrated (photic depth) primary production and integrated chlorophyll concentration
22 in two size fraction (> 2µm and 0.2-2µm). Note the reversal of dates to aid comparisons between
23 figures.

24
25 Fig.5. Changes in the abundance of phytoplankton (a), the concentration of particulate organic nitrogen
26 (PON, b), and the rate of nitrogen assimilation as nitrate and ammonium (c). PON and nitrogen
27 assimilation were measured within the mixed layer at 55% sPAR. Error bars represent one standard
28 deviation for triplicate concentration (b) or rate (c) measurements. Note the reversal of dates to aid
29 comparisons between figures.

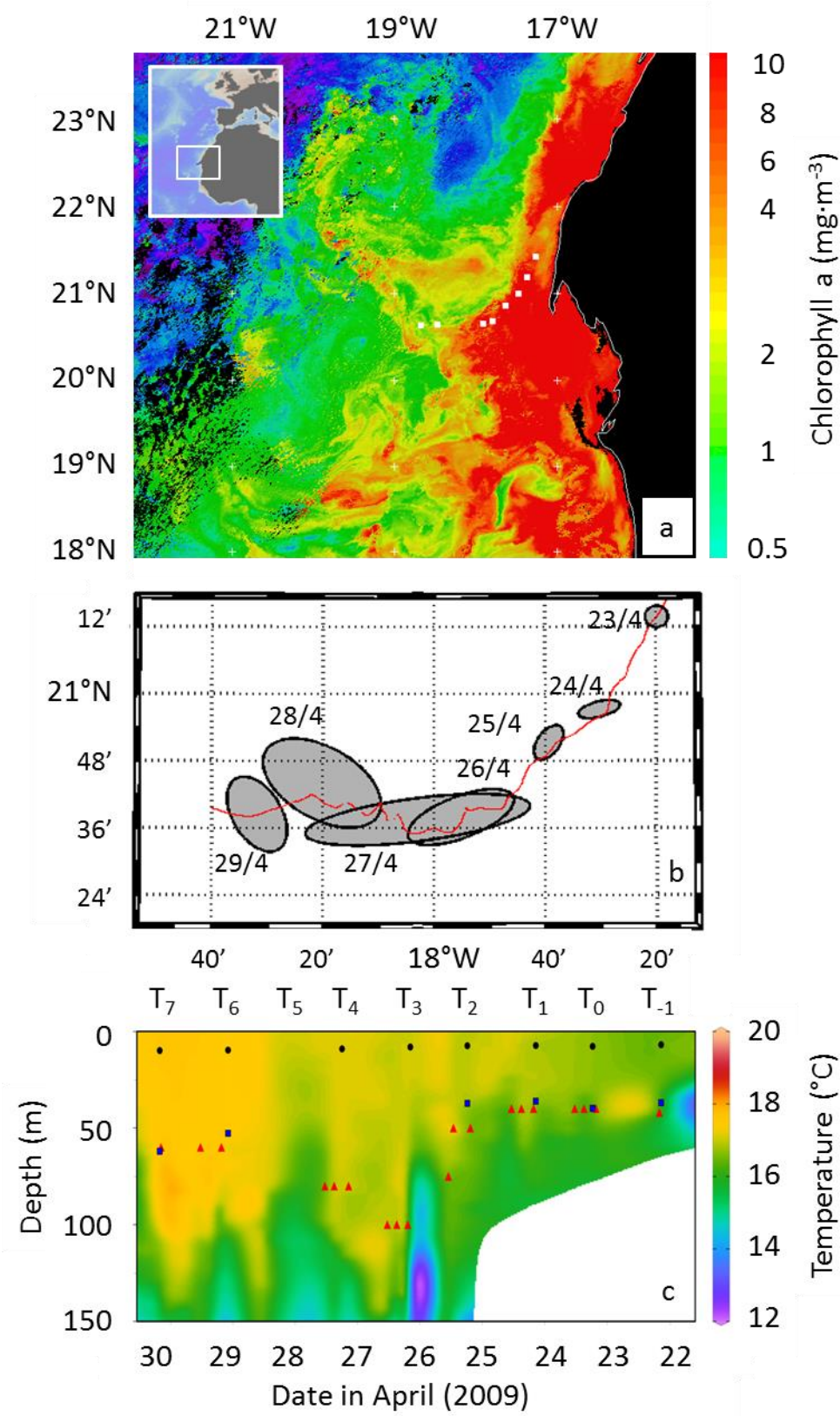
30
31 Fig. 6. Changes in the rate of ammonium regeneration (a), ammonium oxidation (b) and nitrite oxidation
32 (c) for samples taken within the mixed layer depth at 55% and 1% sPAR. Error bars represent one
33 standard deviation for triplicate rate measurements. Note the reversal of dates to aid comparisons
34 between figures.

35
36 Fig. 7. Changes in f-ratio representations (f-ratio; f_c-ratio corrected for isotope dilution due to nitrogen
37 regeneration; f_{regen}-ratio corrected for isotope dilution and the fraction of the nitrate pool represented
38 by 'new' rather than 'regenerated' nitrate. The fraction of the nitrate pool represented by 'new' nitrate
39 is also presented (R_{NO3}). Note the reversal of dates to aid comparisons between figures.

40
41

1 Fig. 1.

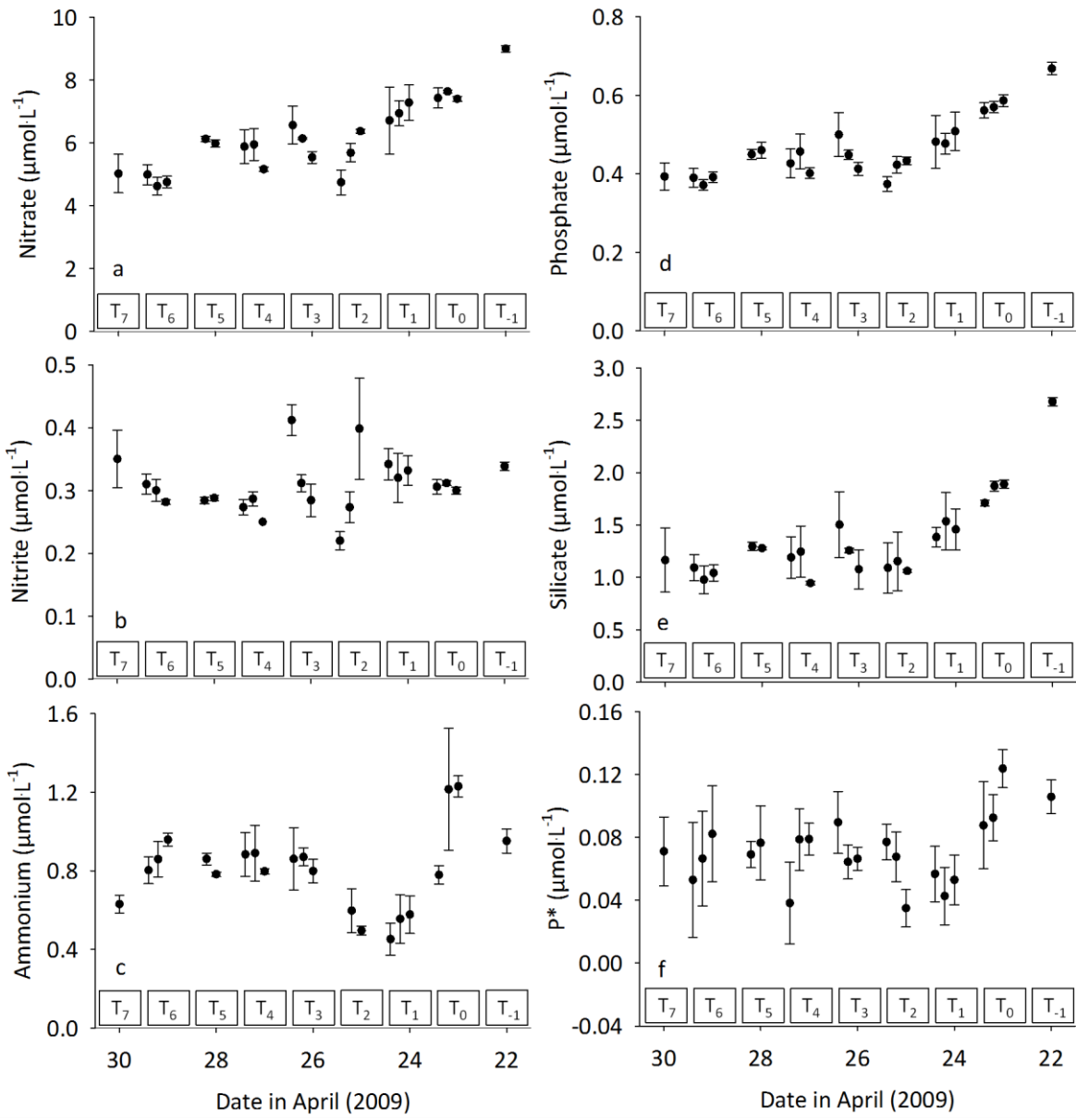
2



3

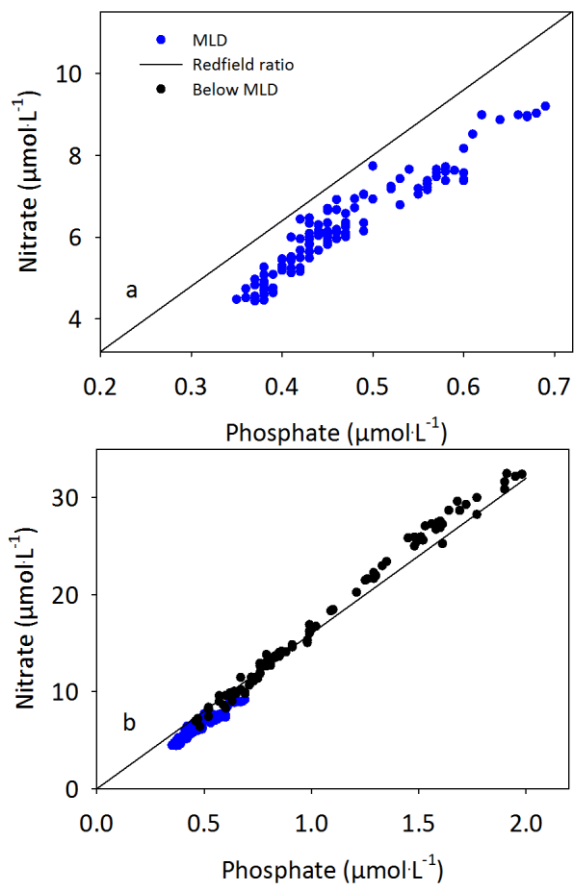
4

1 Fig. 2



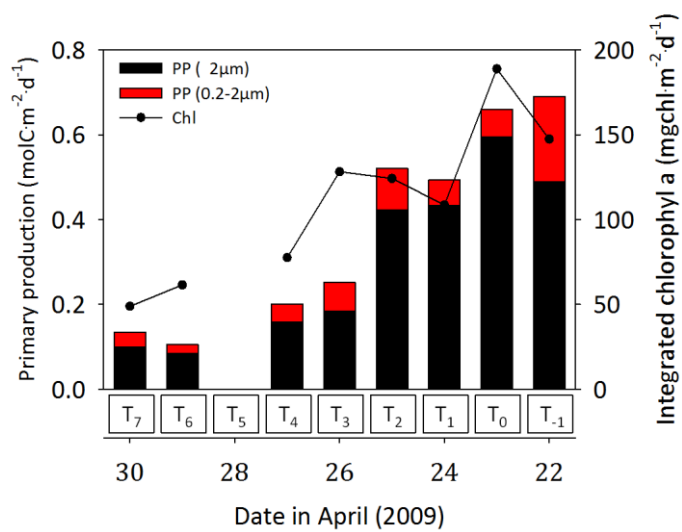
2
3
4
5
6
7
8
9
10
11
12
13

1 Fig. 3



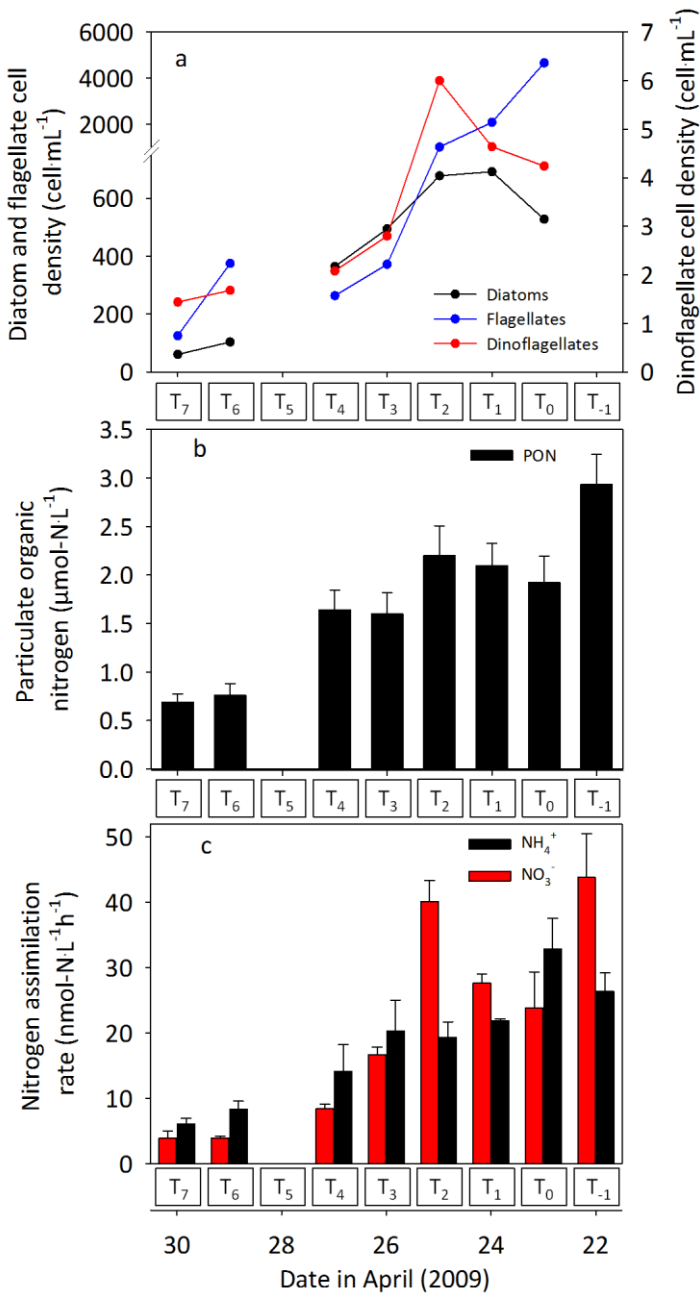
2
3
4

1 Fig. 4



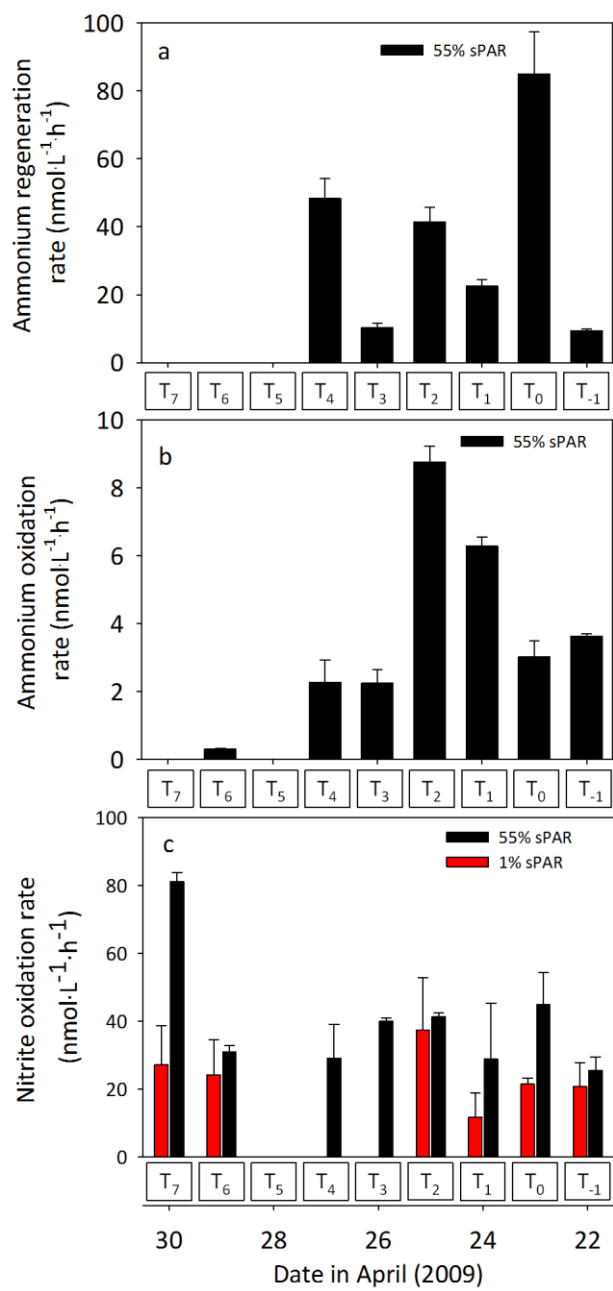
2
3
4

1 Fig. 5



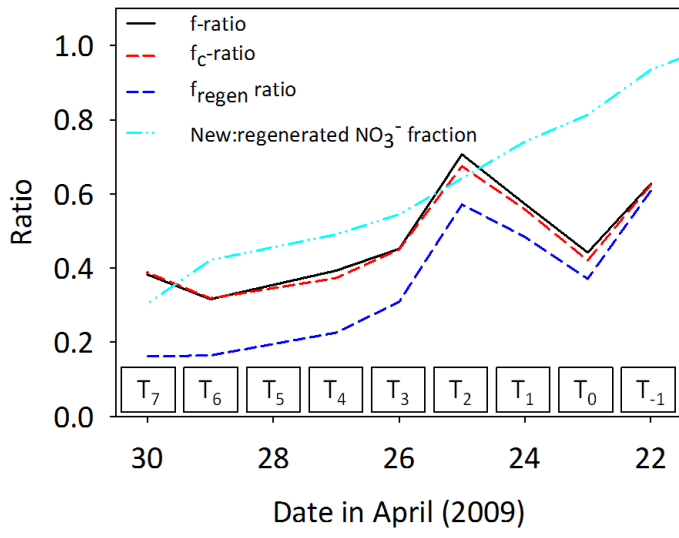
2
3
4

1 Fig. 6



2
3
4

1 Fig. 7



2

3